Characterization of MagneTOF ion detector and Bradbury-Nielsen ion gate

Master's Thesis, 14 May 2018

Author:

Antti Takkinen

Supervisor:

Tommi Eronen

UNIVERSITY OF JYVÄSKYLÄ

DEPARTMENT OF PHYSICS

ABSTRACT

Takkinen, Antti
Characterization of MagneTOF ion detector and Bradbury-Nielsen ion gate
Master's thesis
Department of Physics, University of Jyväskylä, 2017, 41 pages

Multi-reflection time-of-flight mass-separator (MR-TOF-MS) is a high resolution ion mass separator and measuring device. Construction of such a device began in 2016 at IGISOL facility in the accelerator laboratory of University of Jyväskylä. This thesis explored the operation of the MagneTOF ion detector and Bradbury-Nielsen ion gate, both of which will be integral part of the device. An off-line test setup was built to test both the ion gate and the MagneTOF detector using a potassium-rubidium-caesium surface ion source. Appropriate operating voltages for the detector were successfully determined and the output signal from the detector responded well to expectations. Ion gate characteristics were studied by comparing the measured time-of-flight for ions with calculated values. Also, the minimum time in which the gate can be switched from fully closed mode to fully open, and vice versa was determined.

Keywords: IGISOL, MR-TOF, MagneTOF, Bradbury-Nielsen gate

TIIVISTELMÄ

Takkinen, Antti
MagneTOF ioni-ilmaisimen ja Bradbury-Nielsen -ioniportin karakterisointi
Pro gradu -tutkielma
Fysiikan laitos, Jyväskylän Yliopisto, 2017, 41 sivua

Moniheijastava lentoaikamassaerotin (engl. Multi-Reflection time-of-flight mass separator) on korkearesoluutioinen ionien massojen erotteluun ja mittaamiseen käytettävä laitteisto, jollaisen rakentaminen aloitettiin syksyllä 2016 kiihdytinlaboratorion IGISOL-ryhmässä. Tässä tutkielmassa kartoitettiin laitteistoon liitettävien MagneTOF ioni-ilmaisimen ja Bradbury-Nielsen -ioniportin toimintaa. Ilmaisinta käytetään laitteistolla eroteltavien ionien havaitsemiseen ja ioniportin avulla kiinnostuksen kohteena olevat ionit voidaan erotella muista hiukkasista. Tyhjiökammioon rakennettiin koeasetelma, jolla voitiin testata sekä ioniportin että MagneTOF-ilmaisimen toimintaa käyttäen samanaikaisesti tuotettuja kalium, rubidium, ja cesium ioneja. Ilmaisimen valmistajan ohjeistamat mittaukset sopivan käyttöjännitteen määrittämiseksi suoritettiin onnistuneesti ja ilmaisimesta saatu signaali vastasi hyvin odotuksia. Ioniportin ominaisuuksia tutkittiin vertailemalla mitattuja ionien lentoaikoja laskennallisesti määritettyihin. Myös aikaa, joka tarvitaan portin täysin avaamiseen ja sulkemiseen, tutkittiin.

Avainsanat: IGISOL, MR-TOF, MagneTOF, Bradbury-Nielsen ioniportti

CONTENTS

1 INTRODUCTION

In the field of experimental nuclear physics high precision atomic mass measurements have been in the spotlight for the past two decades after introduction of Penning traps [1]. These devices provide very precise atomic mass values down and beyond parts-per-billion (10^{-9}) level. Currently, all major radioactive ion beam facilities like ISOLDE at CERN have them. Even though Penning traps provide the best precision in mass measurements, they are somewhat slow and thus are limited to nuclei with lifetimes of about 10 ms or longer. Separation by time-of-flight is another option for mass separation and spectrometry. Specifically, multi-reflection time-of-flight (MR-TOF) mass separators are complementary to Penning traps due to their fast measurement cycle [2]. Over the past decade these devices have been introduced at radioactive ion beam facilities. Few different types of designs have been developed and currently they are in operation at ISOLTRAP at CERN, University of Giessen, Germany and in RIKEN, Japan [3, 5, 6]. Since their introduction, similar separators have been and are being built on other facilities as well.

Despite differences in experimental setups, all facilities working with short-lived exotic nuclei have to overcome similar challenges. Availability of pure ion ensembles is essential requirement for high-precision mass measurements. Typically contaminants overwhelm by orders of magnitude and thus a separation is essential. For example in Penning trap mass spectrometry, Coulomb interactions between contaminants and the ions of interest cause unwanted systematic effects. This is why elimination and ability to separate contaminant species is the most important quality to aim for. Furthermore, separation of isobaric contaminants should be as fast as possible in order to to avoid decay losses. For this purpose, the MR-TOF can serve as a pre-separator for Penning traps. An MR-TOF can also be used independently as an ion mass spectrometer. Although MR-TOF spectrometers can't currently reach as good precision as Penning traps, they are fast devices and are suitable for nuclei with very short lifetimes [3, 4, 5].

An MR-TOF is an electrostatic device consistsing of two electrostatic mirros and an electric field free drift section between the mirrors. General operation principle of an MR-TOF is fairly simple: charged particles with constant kinetic energy trapped inside the device fly along a multiply folded path. Ions with different masses have different revolution times leading mass separation in time. In other words, ions are set to bounce between the two electrostatic mirros for certain number of revolutions and then finally extracted to an ion detector, where ions' time-of-flight is recorded. Differences in TOF reveal the mass difference of ions.

Thus, for an efficient MR-TOF device the detector measuring the TOF differences to ions is an essential element. In this thesis work the commissioning and basic features of the modern MagneTOF electron multiplier detector are studied [7]. This ion detector is manufactured by ETP Ion Detect company. Ion detectors used in various TOF detection systems are all based on the same phenomenon of charged particles moving within electric and/or magnetic fields. Within the detector, the signal from ion impact must be amplified in order to generate a detectable output signal. The actual ground work for particle

detectors was made in the 1960's by G.W. Goodrich and W.C. Wiley [8]. Their research led to the first commercial TOF measurement system, the channeltron detector and the microchannel plate (MCP) detector. Both are still a well-known and commonly used detector types in any application requiring ion detection [9]. The weakness of these early detector designs was that each dynode surface had to be the same size as the input aperture. Due to today's input aperture size requirements it would cause the detector in question to be impractical in size to many of the systems. In addition, the development work has been driven by the need for really fast detectors and by the improvements in data processing with more powerful computers. The MagneTOF detector manufactured by ETP Ion Detect results from the product development work done in the late 1990's and early 2000's. This detector type uses non-uniform magnetic field for inter-dynode electron transfer. The most important advantage that led to the choice of MagneTOF detector over the more traditional MCP detector in this thesis work was MagneTOF's fast recovery after a large ion burst. That way, ions entering the detector right after a large single ion pulse are also detected. This feature is especially important when contaminant ions are lighter by mass and thus enter the detector earlier due to their higher velocity *i.e.* shorter flight time. A more detailed description of the detector's operating principles and features can be found in section 2.2.3.

The MR-TOF device will be used primarily as a mass separator at IGISOL. For this purpose, a fast and efficient ion shutter is required. That way it is possible to choose which of the MR-TOF-separated ions are to be let forward for measurements and which will be excluded. The fastest device for this purpose is a Bradbury-Nielsen gate (BNG). In 1936, Norris Bradbury and Russel Nielsen came up with the original idea for the BNG [10]. That time the ion gate was primarily developed for studies investigating the movement of charged particles in gas. Since then, multiple versions of the gate have been manufactured for a variety of specific applications and it has also been found to be suitable for time-of-flight mass spectroscopy [11]. The basic principle of the gate is that two interleaved set of wires are set to voltages equal in magnitude but opposite in polarity. The gate is mounted perpendicular to the flight path of ions. When ions fly through the gate and voltages are turned on, the potential field is such that the ions are deflected away from their initial flight direction.Without voltage application, the desired ions will fly through the gate without deflection.

The commissioning of the new MagneTOF detector and the BNG were studied in this thesis work. The gate was included in the test assembly inside MR-TOF vacuum chamber and the goal was to investigate whether the gate could meet the requirement for high time resolution in MR-TOF operations. A more detailed description of the BNG geometry and the operating principle is given in section 2.2.4. For both the BNG and the MagneTOF detector, the experimental arrangement built in summer 2017 is presented in section 3 and the results obtained during the off-line measurements are found in chapter 4. In section 5 this work is considered as one intermediate stage within the MR-TOF project and some future prospects are pointed out.

2 PROJECT BACKGROUNDS

Successful experimental nuclear physics research requires constant development work. One aspect is to broaden the availability of different radioactive ion beams. This is often accompanied with increased amount of co-produced contaminants. The other aspect is the measurement device itself to make it more sensitive, more accurate etc. In IGISOL facility at the accelerator laboratory of University of Jyväskylä, where high precision atomic mass measurements are performed for short-lived nuclei, the next step to reach more exotic nuclei is the installation of an MR-TOF separator/spectrometer. The development work and characterization of the MR-TOF device will be performed separately from the main IGISOL production facility. But its installation and operation as a part of the JYFLTRAP setup requires understanding of both the radiofrequency quadrupole (RFQ) cooler-buncher preceding the MR-TOF and the Penning traps following it. Fixed elements within IGISOL set boundary conditions for the design of new devices. Computer simulations including different parts of the system, together with user experiences, gives an idea what kind of settings are needed to get the MR-TOF integrated to the system. This section first introduces IGISOL basic features and then focuses on principles of the MR-TOF device, including the MagneTOF detector and the Bradbury-Nielsen ion gate.

2.1 SHORT OVERVIEW OF IGISOL IV

Ion Guide Isotope Separator On-line (IGISOL) facility, which was developed in the early 1980's, can be described as a method in which nuclear reaction products are stopped into a gas volume and extracted as ions without a need for an ionization step [12]. Current version of IGISOL-setup in the accelerator laboratory of University of Jyväskylä is the fourth in order. Main research methods are: collinear laser spectroscopy, mass spectrometry and decay spectroscopy. Besides basic research on nuclear physics, IGISOL-group has also been one of the pioneers developing new research techniques [12]. In this section some of the IGISOL-laboratory equipment and functions are briefly discussed in the context of the oncoming MR-TOF analyzer setup.

IGISOL layout is shown in figure 1. The ground floor houses the vast majority of the equipment. In addition, there is an ion source for producing stable ions on the 2nd floor and target chamber pumping station in the basement. One of the two available cyclotrons is utilized for producing short-lived ions at IGISOL. The newer MCC30/15-cyclotron is located in the same wing of the building with IGISOL (also seen in Figure 1) and the other cyclotron, K130 is located in the older part of the accelerator laboratory.

In some occasions the primary beam from either of the cyclotrons is not available for IGISOL use. For that reason it is essential to have a mode of operation where ions for IGISOL actions are produced by an external ion source. There are many locations to produce stable ion beam for e.g. for tuning and characterizing the MR-TOF. Also, on-line measurement cycles are optimized as succesful preliminary work for experiments can be done before the valuable beam time with the cyclotron starts.

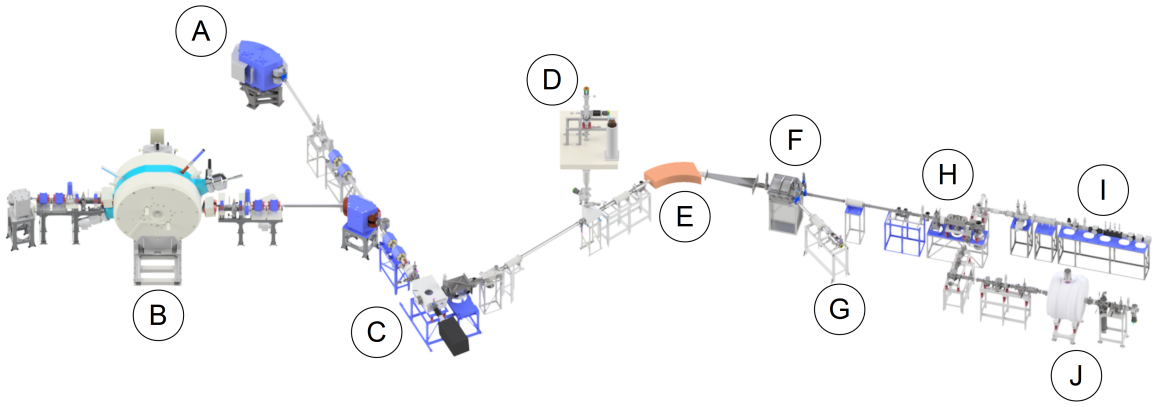

Figure 1: IGISOL layout. The labels are as follows:

A Beamline from K130 cyclotron	F Switchyard
B MCC30/15 cyclotron	G Decay spectroscopy line
C Target & gas cell	H RFQ cooler buncher
D Offline ion source (2nd floor)	I Collinear laser spectrocopy line
E Dipole magnet	J Penning traps

For any short-lived ion production, the primary beam from the cyclotron is directed into a target. Products from reactions between incoming primary beam particles and target material are primarily slowed down in the target material. The final stopping happens in helium gas where their charge state is typically reduced to +1 or +2 due to charge-exchange reaction with helium gas. The ions are extracted out from the gas cell with the gas flow and enter a radio frequency sextupole Ion Guide (SPIG), which keeps ions focused. The beam of ions continue to the extraction chamber where they are accelerated with 30 kV voltage. Next, the beam is guided through a 15° electrostatic bender and a 55° dipole magnet, which makes coarse mass separation (atomic mass number selection) as it can be tuned for specific mass-to-charge ratio. As the beam enters the electrostatic switchyard, which is simply a vacuum chamber containing necessary ion optical elements to bend the beam to one of the three beamlines.

The centermost of the lines from switchyard leads to the Radio Frequency Quadrupole (RFQ) cooler-buncher which is a linear ion trap filled with helium buffer gas [13]. The continuos beam from IGISOL can be collected inside the RFQ device into a potential well and sent onwards as short ion bunches or, alternatively, as continuous beam as well. Reduction of the energy spread and cross sectional spatial spread of the beam, in other words cooling the beam, is obtained by harnessing both a static electric field and an alternating radiofrequency (RF) field inside the RFQ. Currently, the RFQ produces ion beams with low energy spread ($<$ 1 eV) but rather long temporal spread ($\sim$ 10 µs). For MR-TOF operation, the energy spread would be excellent but the temporal spread is horrible. Thus, extraction side properties of the RFQ needs to be modified in order to have decently time focused ion beams ($<$ 100 ns) for MR-TOF operations. This development work is already in progress while writing this thesis report. More specific description related to RFQ features can be found in Refs. [13, 14].

From RFQ, the ions will be sent left towards the collinear laser spectroscopy line or to right towards the Penning traps. The MR-TOF device presented in this thesis will finally be located in the line after the RFQ leading to the Penning trap [15]. To fully integrate

the MR-TOF to the system, RFQ extraction side ion optical elements need also to be studied and optimized first with computer simulations. Finally, the whole setup needs to be commissioned and characterized with real ions.

2.2 MULTI-REFLECTION TIME-OF-FLIGHT MASS SEPARATOR

2.2.1 Overview of MR-TOF designs

There are many different kinds of solutions for time-of-flight mass spectrometers (TOF-MS) worldwide. Linear and singly-reflecting TOF-MS devices are the simplest instrumental solutions. Though, they are limited in the mass resolving power because of the short flight path length for ions and different initial properties of incoming ions. By re-using the flight path inside the device the mass resolving power of the separator/spetrometer is appreciably improved.

Currently, there are three "competiting" MR-TOF-MS designs with two sets of reflector electrodes and a closed ion flight path in between to be used for mass measurements and separation of short-lived ions. One is developed at Justus-Liebeg-University Giessen Germany, one at RIKEN, Japan and the third at University of Greifswald, Germany. The MR-TOF device developed in Greifswald is in use at the ISOLTRAP facility at CERN in Geneva [5]. The IGISOL MR-TOF presented in this thesis report is heavily based on the work done by Wolf *et.al.* at ISOLTRAP [3, 4].

There are few different approaches for MR-TOF device geometries and they can be categorized according to their symmetry, the number of electrodes used in the reflection regions and ion optical design [5]. In this context, symmetric geometry refers to a solution which has two identical mirror sets. If there are any differences between the mirrors, the analyzer is said to have an asymmetric structure. Typically, the number of electrodes varies from four to eight within each mirror set. At IGISOL, six electrode configuration was chosen in the same way as it was at ISOLTRAP.

Other properties defining different types of MR-TOF analyzers are ion injection/ejection procedures, time focus matching, time-of-flight detecting and mass separating operations. Generally, there are two different ways for ion injection and ejection with an MR-TOF. In conventional method, mirror potentials are pulsed in order to trap ions inside the device and after certain number of revolutions accelerate them out of it. The other option is to use electrostatic mirrors combined with an in-trap lift electrode which is then pulsed [3, 4, 5]. The latter is the method of choice at IGISOL and it will be discussed in more detail in the following section 2.2.2.

In principle, the goal is to make an MR-TOF device as isochronous as possible to the energy spread of the ions. By saying this, it means that after a number of revolutions the ions still have the same time focus for all ions. Only difference in time then comes from different mass of the ions. Conventionally, the time focus can be tuned by changing voltages of the mirror electrodes. Other options for controlling positioning of the time-focus plane are to change the voltage setting for the in-trap lift electrode or to use a post-analyzer planar reflector, described in Ref. [5]. Also this feature is further discussed in the next section 2.2.2 in the point of view for IGISOL MR-TOF design.

When using a MR-TOF device for mass measurements an ion detector is placed at the time-focus plane. In ion beam purification purposes when MR-TOF is used as a mass separator, a fast ion deflector is installed at the time-focus position. In most cases it is

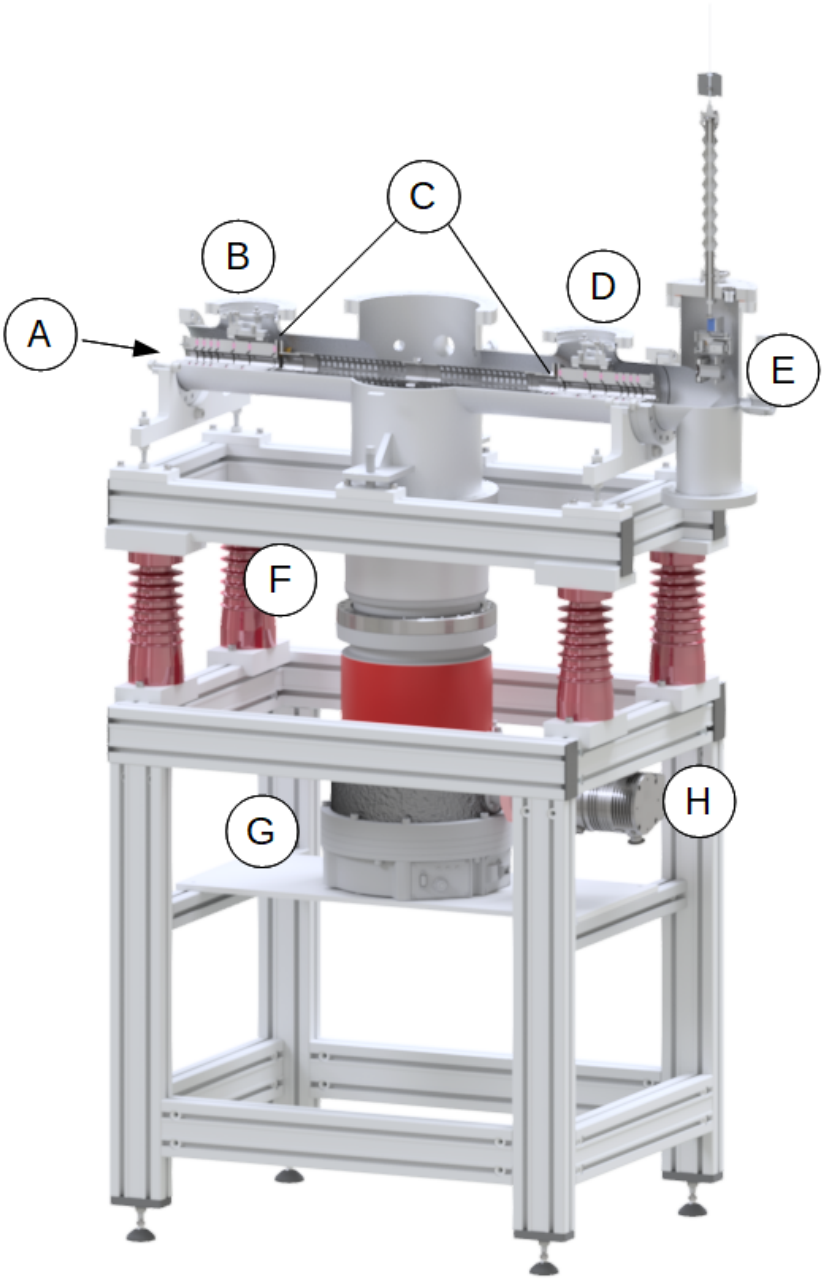

Figure 2: MR-TOF main parts.

A Ions from RFQ	E Exit side chamber: MagneTOF and BNG
B First electrostatic mirror	F Ceramic insulator
C Drift section	G Vacuum pump (STP-iXR1606)
D Second electrostatic mirrror	H Pre-pump (smaller turbo pump)

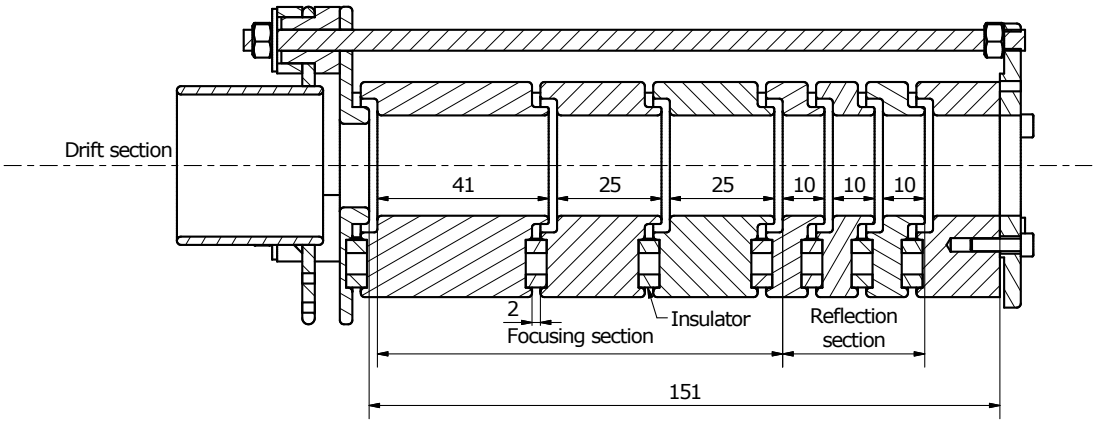

Figure 3: Cross-sectional view of electrostatic mirror set.

practical to use a linear actuator arm that has both the ion detector and the Bradbury-Nielsen gate attached. This way it is quick to switch between ion detection and mass separation modes by changing the position of the holder.

2.2.2 Operation principle

Particles with different masses m_i at a potential U (with respect to the extraction beamline potential) extracted from the RFQ towards the MR-TOF gain kinetic energy

$$(1) \quad E_{kin} = z_i e U = m_i {v_i}^2/2,$$

where z_i is the charge state of ions (commonly +1), v_i is their velocity and e is the elementary charge. Since these ions have the same flight path, it holds that their time-of-flight t_i becomes mass and charge dependent:

$$(2) \quad t_i \propto {v_i}^{-1} \propto \sqrt{m_i/z_i} \ .$$

When ions are flying at constant electric potential, their velocity v is

$$(3) \quad v = \sqrt{\frac{2eU}{m}}$$

and time-of-flight t over distance s is

$$(4) \quad t = \frac{s}{v} = \frac{s}{\sqrt{\frac{2eU}{m}}} \ ,$$

How well an MR-TOF performs as a mass separator or spectrometer is determined by the time spread, Δt. Mainly this is determined by the energy spread and time spread of

the ion bunch. How well a mass separator performs is commonly quantified with a mass resolving power (MRP or R), defined as [4]

$$R = m/\Delta m = t/2\Delta t \ . \tag{5}$$

It can be improved by increasing the total time of flight t or decreasing the time spread Δt. In practice decreasing the energy spread and the time spread of ion bunches is carried out by modifying properties of the RFQ buncher section. The total time of flight for ions inside the MR-TOF can be extended by decreasing the average kinetic energy of ions or increasing the length of the flight path. The former increases the relative kinetic energy spread which is an unwanted phenomenom because it leads to larger time-of-flight dispersion with respect to energy. Extending the flight path *i.e.* the number of revolutions for ions in the MR-TOF increases the time-of-flight difference between ion species. Maximal separation is reached when the ion species are half a cycle apart [3]. The time difference between ions species i and j at revolution number n can be written as

$$\Delta t_{ij} = n|T_i - T_j|, \tag{6}$$

where T_i and T_j are individual revolution times for different ion species. Maximal separation is when

$$\Delta t_{ij} = \frac{1}{2} T_i \ . \tag{7}$$

MR-TOF device's main parts are shown in figure 2. As it was mentioned earlier, based on previous works (R.N. Wolf, W.R. Plass) and simulation results a six-electrode mirror configuration was chosen for the JYFL MR-TOF setup. This system is cylindrically symmetric and the full length is about 80 cm. Insulators with 4 mm thickness are placed between the electrodes to create 2 mm gaps between the electrodes. It is possible that these insulators might have minor charges as well. That is why electrodes were designed to have L-shaped cross-section wich ensures that the electric potential of the MR-TOF is defined only by the inner surfaces of the electrodes and any patch charges on the insulators and support structures will not affect the field. The dimensions of electrodes that affected the most on flying particles' trajectories according to computer simulations were the length of each electrode in the direction of the beam axis and inner diameter of the electrodes. Simulations carried out with electrodes of equal lengths indicated the necessity to have three types of components. This was due to the fact that only rather modest mass resolving power could be produced when using electrodes that have about same length. Various electrode sizes were tested. Modifying electrodes gradually from one simulation to another mainly intuitively changing lengths of the electrodes led to a combination that produces mass resolution of about $R = 2.4 \times 10^5$ for ions with 1 keV energy while the voltages on the mirror electrodes with respect to the drift tube were within $\pm$ 2 kV. The first electrode just next to the drift tube was 41 mm in length,

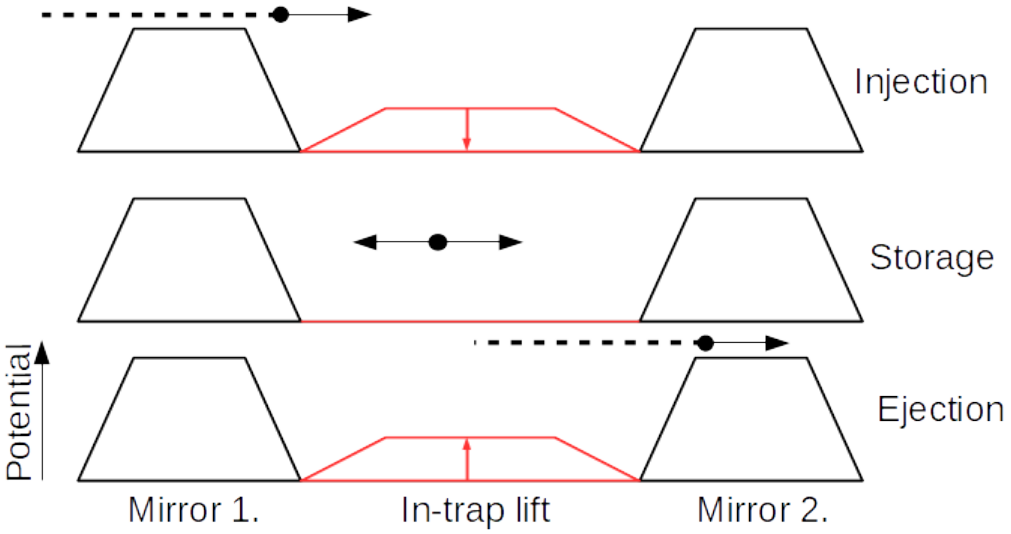

Figure 4: Ions are trapped inside the MR-TOF device by using the in-trap lift electrode. In the top row the pulsed drift tube has potential U_{lift} and ions are injected into the MR-TOF through the first electrostatic mirror. When the drift tube is pulsed to ground potential in the middle row, ions get trapped inside. At the bottom of the figure ions are extracted out of the MR-TOF section by pulsing drift tube potential back up.

the following two were 25 mm and the last three were 10 mm long. Inner diameter from 16 mm up to 32 mm for the reflector electrodes were tested and the highest mass resolution mentioned above was achieved by using 24 mm. Cross-sectional view of the MR-TOF mirror electrodes is shown in figure 3.

From RFQ cooler-buncher, the ions have to be injected into MR-TOF by guiding them through the entrance mirror. Similarly, after a certain number of reflections, the ions are ejected through the exit mirror for further investigations. Criterion for both injection and ejection is that the total ion energy (kinetic + potential) has to be positive in the mirror region. This is in contradiction to the trapping mode of the device [3]. In conventional method the entrance mirror electrodes are pulsed to lower potential so that the ions are able to pass to the drift section. When the ions enter the drift section, the entrance mirror is raised back to higher potential. Thus, ion bunches get trapped inside the device. Similarly, the potential of the exit mirror can be pulsed to lower potential for ion ejection. However, in this work this approach is not used to avoid rather complicated stabilization of switchable kV-level voltage supplies [3, 5]. Instead, the mirror electrodes are kept at of static potentials while the drift section acts as an in-trap lift. The incoming ions must have their total energy positive in the entrance mirror region, where electrodes have up to 2 kV higher potential than the drift section. This way, the ions are able to pass the first mirror in the entrance region and enter the drift tube which is kept at potential U_{lift} to reduce ions' kinetic energy. Once the ions have entered the lift, the potential of the lift electrode is now quickly switched to ground potential. Consequently, the potential of the ions is lowered by U_{lift} and their energy is no longer high enough to pass the mirrors, *i.e.*, they are trapped. Similarly, when extracting ions, the in-trap lift voltage is activated again while the ions are in the drift tube, they regain enough energy to pass the electrostatic mirrors. Thus, the ions are ejected out of the device through the exit mirror region [16]. Operation principle for MR-TOF ion trapping is shown in figure 4. For ion beam purification purposes MR-TOF needs to be used in combination with a fast

temporal ion gate. This is realized by placing a Bradbury-Nielsen ion gate [10] right after the MR-TOF device on the way to the Double Penning trap.

2.2.3 MagneTOF DM291 ion detector

The ion detector purchased for the MR-TOF analyzer use is called by the trade name 'MagneTOF DM291'. There are few different models available for this detector, and there are also some optional features for each product. The detector is shown in figure 5. Its entrance aperture size is 10×25 mm and the transmission effiency through the outer grid is about 92%. Electrical connections can be made in couple of different ways. For a non-floating system it is really simple: the positive high voltage pin visible in the lower left corner in the figure is connected to ground potential and the negative operating voltage supply is connected to the pin on the left bracket of the detector [7]. Detector's charasteristics include its aging over time, which in practice means the need for higher operating voltage values [17]. Initially, the appropriate operating voltage for a new detector is around 2500 V and for an aged detector it is allowed to rise up to a maximum voltage of 4000 V. At the end of its operational life the detector draws a current of ~ 300 µA from the high voltage power supply. There is an SMA connector in the middle of the detector's backside, from which the output signal is transferred along a 50 Ω coaxial cable. As a minimum requirement for the vacuum conditions surrounding the detector, manufacturer has indicated 10^{-4} Torr (1.3×10^{-4} mbar). The detector is ready for use immediately after vacuum pumpdown and it does not need time to adapt the conditions. Ion impact surface flatness is ±10 µm and as a optional feature it would also be available in ±5 µm. The special feature to be mentioned for this detector type is the use of non-uniform magnetic field in order to guide the electrons bounced off the ion impact plate towards the second dynode. The number of electrons is amplified from one dynode to another and finally a measurable amouint of charge is obtained. Ion optical arrangement inside the detector is shown in figure 6. Expected output signals from the detector according to manufacturer are 1 ns wide and 30 mV into 50 Ω. Typical operational gain for MagneTOF detector is about 10^6 at operating voltage of 2650 V for new detector.

Absolute detection effiency of about 80% has been reported. In measuring geometry the alignment of the detector is a major factor. Mounting the detector so that its impact surface is as perpendicular to the incoming ion beam as possible is essential for gain. In comparison with the more traditional multichannel plate MCP detector, the MagneTOF detector is expected to be at least as efficient or better. Especially with high ion rate hitting the detector, the MagneTOF detector does not suffer from detector downtime like MCP does. With proper alignment, MagneTOF detector performance may be significantly higher than MCP. There are two optional mounting methods, either from the front or rear side of the brackets. Mounting bolts are made of PEEK plastic and threads are protected with ceramic insulation tubes [7].

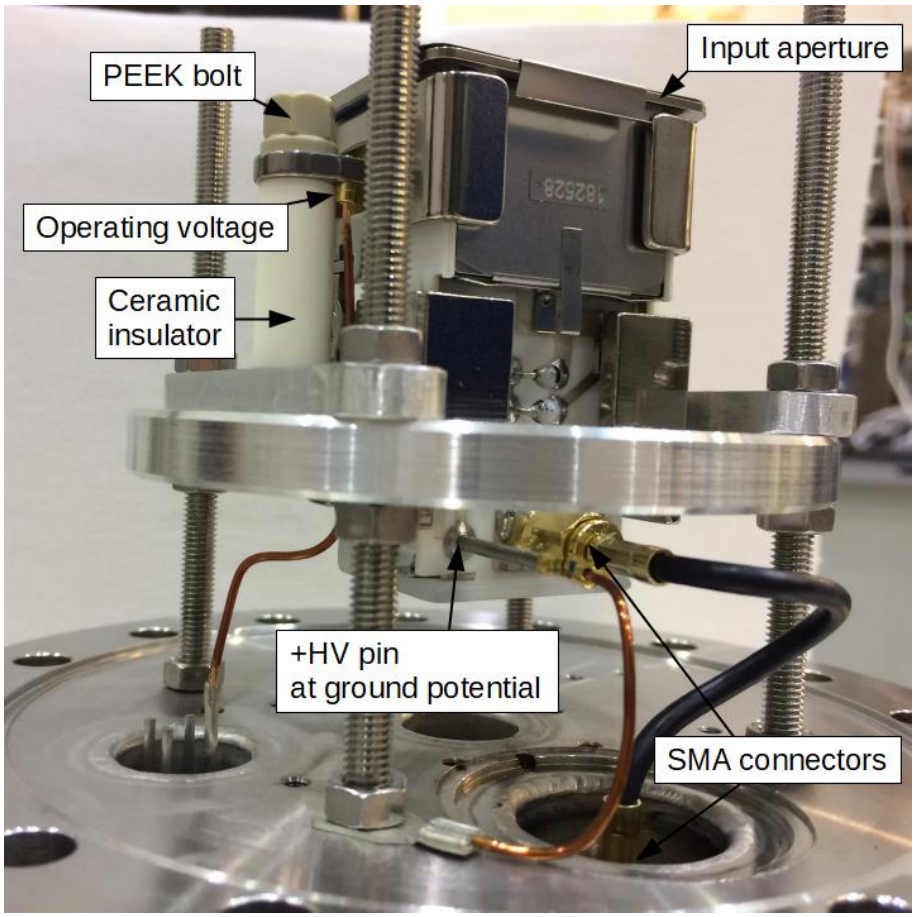

Figure 5: MagneTOF detector attached to a standard CF100 flange.

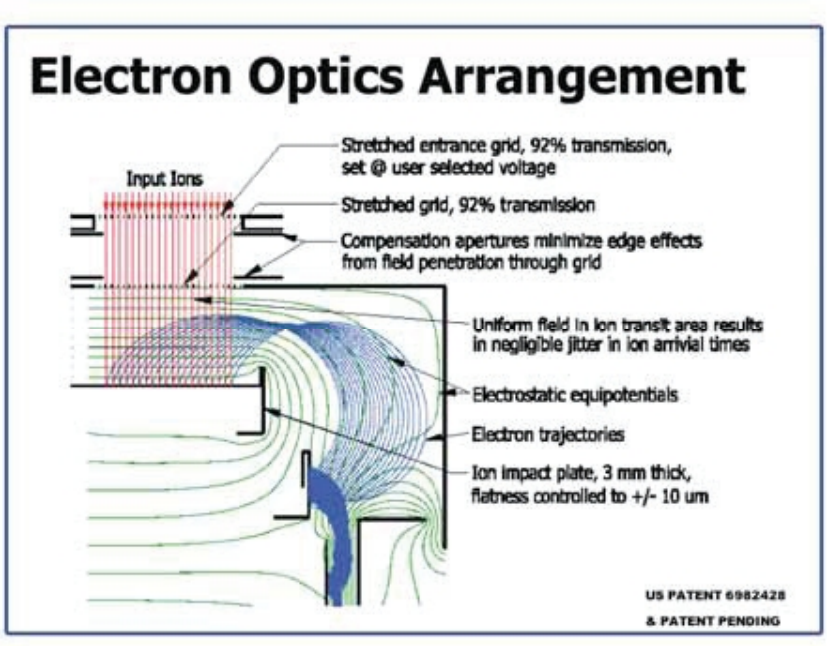

Figure 6: MagneTOF detector ion optics. Figure taken from [7].

2.2.4 Bradbury-Nielsen ion gate

Bradbury-Nielsen ion gates are widely used where fast ion beam on-off switching is required, for example in the fields of electron microscopy, mass spectrometry, and ion motion spectrometry [22]. Such a gate can be used e.g. to chop continuous ion beam to make it of pulsed type or to reject temporally separated ion bunches. A Bradbury-Nielsen ion gate can be constructed in various sizes and shapes and compared to alternative deflection plates it has turned out to be a fairly effective solution [18]. In this context, effiency refers to the short time needed between BNG open and closed modes.

Figure 7 shows a BNG that consists of a frame made of PEEK plastic into which two interleaved and electrically isolated wire sets are attached. Typically electrodes used in most applications are gold-coated tungsten wires with a diameter of less than 50 µm. In practice, the most important feature affecting gate characteristics is the spacing of the wires. Most often wires of 10 ... 20 µm in diameter and spacing around 250 ... 500 µm are used. BNG is mounted so that the plane formed by the wires is perpendicular to the incoming beam axis [19].

Operating principle of a BNG is outlined in figure 8. There are two possible states the gate can be in. When the gate is denoted to be in 'closed' state, the two wire sets within the grid are set to voltages equal in magnitude but opposite in polarity. In this case, the electric field formed by the wires deflects the incoming ion beam into two separate branches. If the angle of deflection is sufficiently steep or the distance long enough, the particles can be guided to collide with vacuum chamber walls and therefore they are not detected further along the beam line. In the other mode, when the gate is denoted to be 'open', the wires are kept in zero potential and charged particles fly through the gate all the way to a detector without experiencing any deflection due to the gate. When the gate is open, its transmission in most cases is between 85% and 98% depending on the diameter of the wires and the spacing. When the gate voltage is switched on, the deflection angle for ions can be derived from BNG's dimensions and wire voltages [20]:

$$\tan\alpha = k\frac{V_p}{V_0} \quad (8)$$

where V_p is the voltage set on the gate electrodes and V_0 is the acceleration voltage for ions. Coefficient k is obtained from the following equation [20]:

$$k = \frac{\pi}{2\ln\left[\cot\left(\frac{\pi R}{2d}\right)\right]} \quad (9)$$

where R is the radius of the cross-section for round wires and d is the distance between neighbouring wires. In addition, the gate can be characterized by determining theoretical capacitance. The equation for capacitance of parallel wires results [21]:

$$C = \frac{N\pi\epsilon_0 L}{\cosh^{-1}(d/2R)} \quad (10)$$

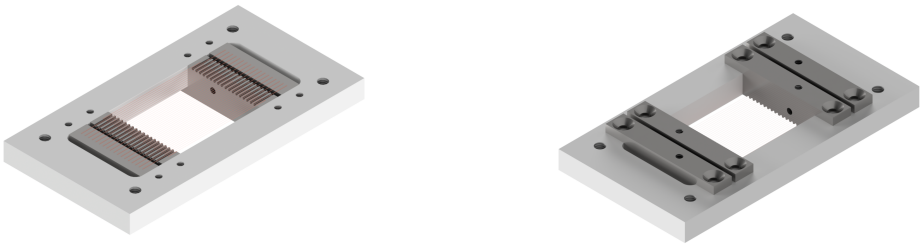

(a) Frontside (b) Backside

Figure 7: Rendered image of BNG with Autocad Inventor Pro 2017.

where N is the number of wires, ϵ_0 is vacuum permittivity, L is the length of wires within the frame, d is the wire spacing and R is the wire radius as in the previous notes above. Bigger the capacitance the more energy has to be drawn from the switch power supplies during voltage switching. The voltage switch device has a small, unavoidable ohmic resistance that slows down voltage changes. Typically, the voltage rises or decreases to 90 % of the maximum set value in about 10 ns time scale.

The main advantage of BNG over an ordinary planar deflector is that the electric field generated by the wires vanishes very quickly outside the gate in the direction of the ion beam axis. This is a consequence of potentials from opposite polarity wires cancelling out each other. More specifically, the deflection region in which the potential field is non-zero extends approximately one wire spacing out from the plane formed by the wires in each direction. Thus, when the gate voltages are switched on the ions pass through the deflection region which has a total lenght of two wire spacings ($2d$). The time-of-flight for ions through this deflection region is a useful factor for characterizing the gate. Variable is known as the residence time τ_{res} in literature and it can be derived from the equation [19]:

$$\tau_{res} = \frac{2d}{v_0} = 2d\sqrt{\frac{M}{2qV_o}}\ , \tag{11}$$

where v_0 is the charged particle velocity, M is the particle mass and q its electric charge.

Since the voltage on BNG wires is pulsed on and off it should be noted that complete deflection or transmission takes place only if ions fly through the deflection region while the gate is set perfectly in either of the alternative modes. The ions that are within the BNG deflection region while the voltages are switched from one state to another experience only partial deflection. This way, ion deflection angles vary at the rising and falling edges of the voltage pulses [20]. Reducing wire spacing narrows the deflection region and leads to better temporal accuracy. An additional advantage of reducing the spacing is that the same deflection angle for ions can be achieved with lower wire voltages. As a drawback, denser spacing will reduce the open area and thus the transmission of the ions through the grid. In addition, dense spacing between the wires makes gate preparation much more challenging. In literature, there are also some recommendations for determining suitable BNG dimensions for different uses. As a rough rule of thumb, the following equation can

be used [19]:

$$(12) \quad d = \frac{\Delta T}{2}\sqrt{\frac{2qV_0}{M}} \ ,$$

where as an addition to previous notes ΔT denotes the required time resolution for the system and q is the ion charge.

In modern day systems the need for higher time resolution and more effective construction as well deconstruction methods guides the development of ion shutters. Thus, several groups have decided to take part in engineering various methods for building BNGs. Mechanical handling of the wires is challenging in itself, as the maintenance of wire tension and taking possible wire breaks into account during construction set the chosen method into a test. Additionally, exact positioning of the wires parallel to each other and electrically separating them makes it difficult to reduce the wire spacing. Besides actual wires as electrodes there also solutions using photo-etched metallic foil grids for BNG [22].

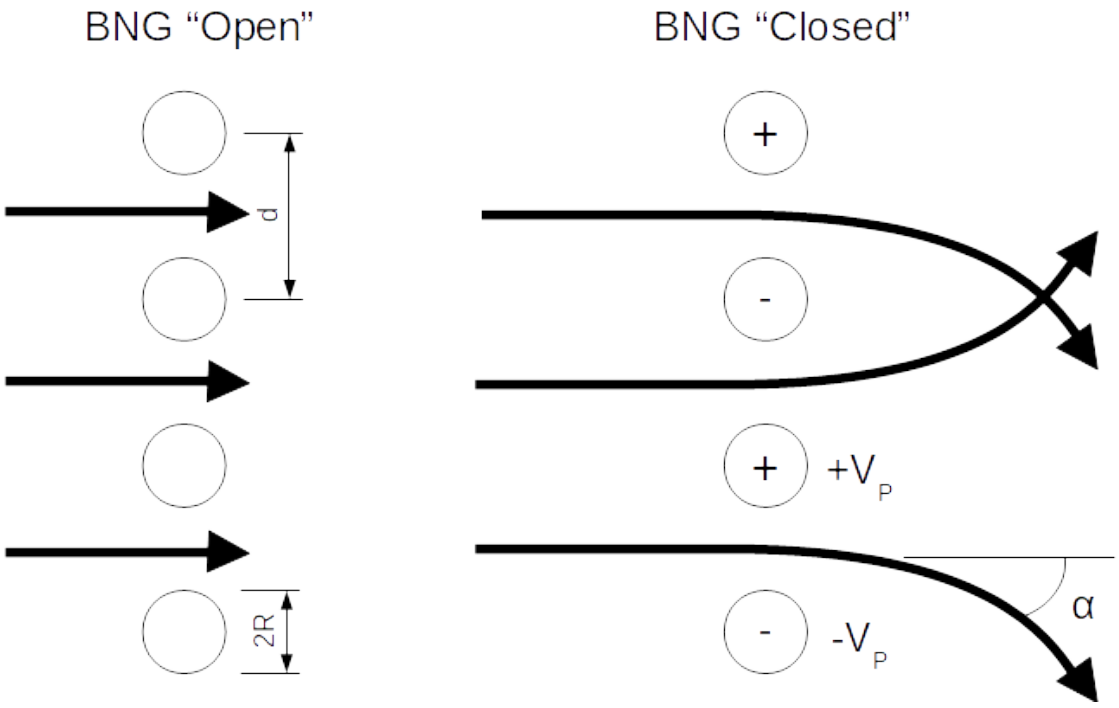

Figure 8: Schematic presentation of BNG operation principle. On the left side the gate is in open mode as wires are at ground potential. When voltages opposite in polarity are applied to the wires, incoming ions are deflected. In this picture, 2R is enlarged for clarity; in reality d >> R. See text for more details.

3 EXPERIMENTAL SETUP

Now that basic features of IGISOL actions, MR-TOF device, MagneTOF detector and BNG have been introduced it is time to have a look at experimental arrangement combining these elements into an off-line test station. First, the BNG constructed at IGISOL is detailed, including information on materials and dimensions chosen. As there are different mounting options for the MagneTOF detector and BNG inside the MR-TOF vacuum chamber the test system geometry is presented after which all the measurements are listed.

3.1 BUILDING A TEST SETUP FOR ION DETECTOR AND GATE

First steps: accessory racks and vacuum system
The setup for testing MagneTOF and BNG was built in to the vacuum vessel of the final MR-TOF device. In practice all outer parts like the vacuum chamber, pump, high voltage insulator and such for the MR-TOF were assembled together and only the inner parts like the electrostatic mirros and the in-trap lift electrode, had to be omitted at this point. The first step was to assemble the supporting aluminum frame for the vacuum setup and accessory racks for the electronics. The vacuum chamber was manufactured in the mechanical workshop of the accelerator laboratory. The whole setup is ultra high vacuum ($p < 10^{-8}$ mbar) compatible with CF flanges. Below the chamber a 30 kV ceramic insulator and powerful 1600 l/s Edwards STP-iXR1606 turbomolecular pump were attached. This way the vacuum chamber can be floated at 30 kV high voltage while the pump is at ground potential. For the final MR-TOF assembly a smaller 65 l/s turbomolecular pump will be installed as a pre-pump for this larger turbo to increase the compression ratio for helium gas. However, in this thesis work the demand for vacuum was not as high and thus the small turbomolecular pump was left out at this point. A 6 m^3/h scroll pump was used as a pre-pump. Schematic drawing 9 demonstrates all the key components of the test setup and figure 2 shows the setup itself.

BNG geometry
The Bradbury-Nielsen ion gate manufactured at IGISOL has a rectangle-shaped PEEK plastic frame with width of 65 mm, length of 35 mm and thickness of 5 mm (see Fig. 7). 20 µm thick gold coated tungsten was used for the wires. Two pairs of metal rails with width of 5 mm and 1 mm gap between each other were attached to the rear of the gate frame. The wires were spot welded to the metal rails so that wire spacing was set to 500 µm. Each wire is in contact with one of the metal rails so that every other wire is at the same potential. Metal rail pairs and hence also the electrode sets are electrically isolated from each other. Maximum window size for IGISOL BNG grid is 22 mm times 20 mm resulting area of 440 mm^2. 20 µm thick wires with 500 µm spacing results in 96 % transparency.

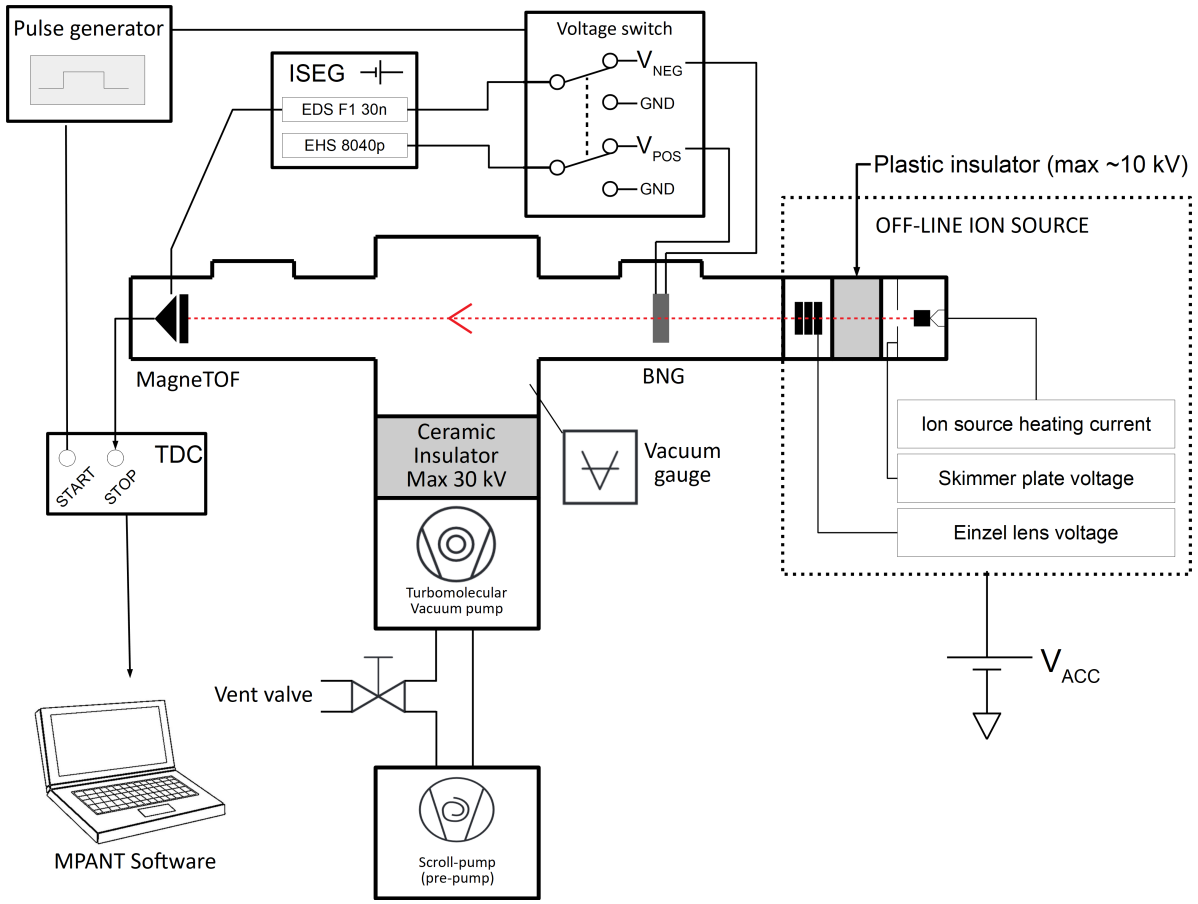

Figure 9: The Bradbury-Nielsen ion gate and the MagneTOF detector were mounted inside the MR-TOF vacuum chamber for off-line tests. The flow of ions in the drawing is from right to left, shown by the dashed red line.

For these test measurements the size of the gate window was limited by circular collimators. For this purpose, $\sim$ 1 mm thick aluminum plates with holes of 1 cm in diameter were mounted on both sides of the BNG support frame. This way the wire grid surface visible for incoming ions had area of 79 mm^2. Figure 10 shows a BNG attached onto a standard CF100 flange. Some extra electrical shielding was added to the front of the wires feeding voltages to BNG. By using the mounting method described here the BNG was placed in the front end of the vacuum chamber close to the off-line ion source. Distance between the BNG and the MagneTOF detector was 635(5) mm.

MagneTOF detector positioning

In the test assembly, cylindrical collimators were installed between the off-line ion source chamber and the main chamber and also to the front of the MagneTOF detector. The aim was to have as parallel beam as possible and to limit the number of stray ions ending up to the detector and thus to minimize faulty observations. This especially concerns the ions within the gate when the gate voltage is switched: ions with bigger angle might get deflected just right to end up to the detector. The MagneTOF detector was mounted to the far end flange of the MR-TOF vacuum chamber, opposite to the ion source. The MagneTOF detector has mounting brackets on the front face of the detector. As shown in figure 5, the detector was attached to the adapter ring, which in turn was fixed onto the CF100 flange with rigid four-point geometry using M5-size threaded rods. Aligning the

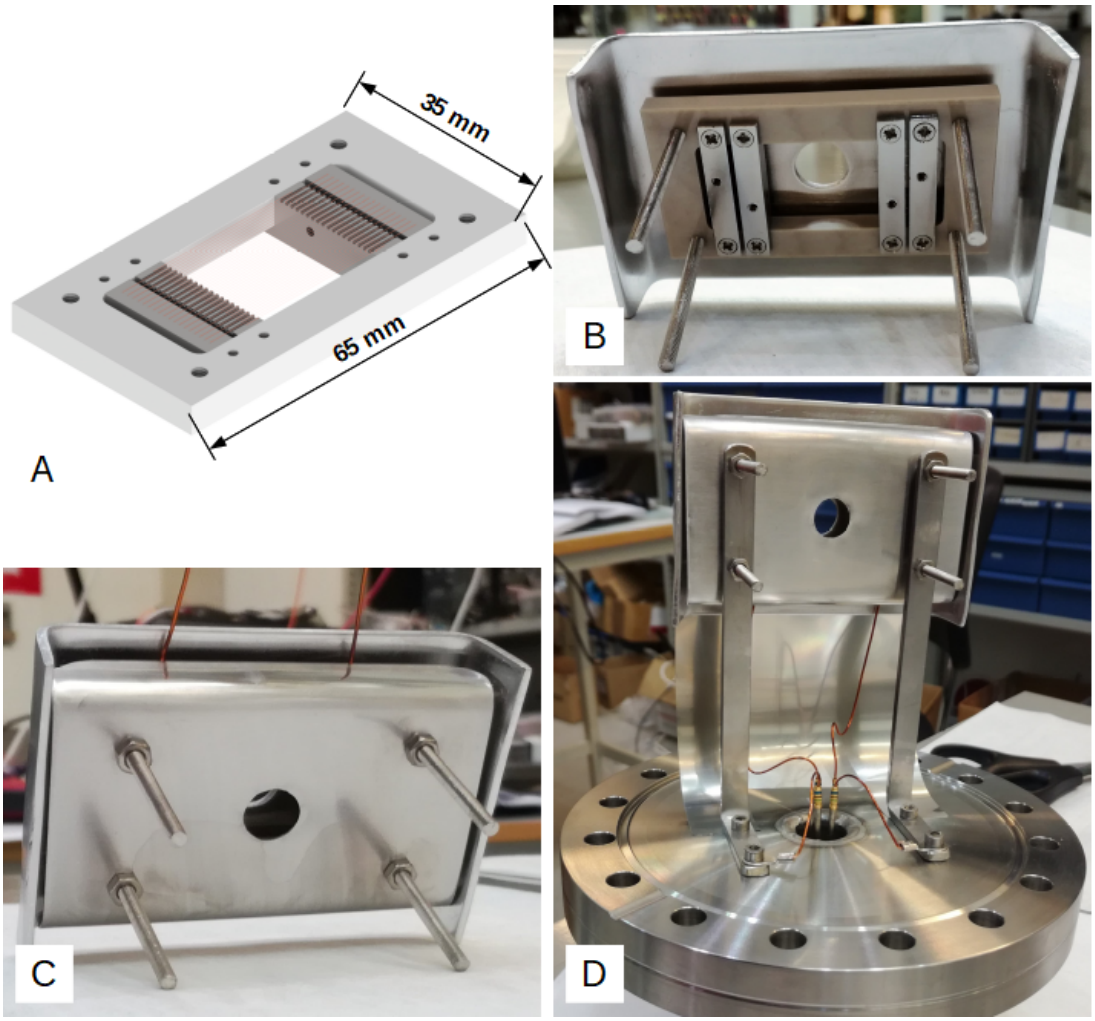

Figure 10: IGISOL version of the Bradbury-Nielsen ion gate attached onto CF100 flange. A) Rendered image of the gate; B) backside when the frontside steel case is attached; C) backside when the backide casing is mounted; D) the gate mounted on a CF100 flange with voltage feedthroughs attached.

detector face to be perpendicular to the incoming ion beam was performed by measuring distance from the adapter ring to the flange face. Two electrical vacuum feedthroughs were installed: one rated up to 6 kV to supply the negative operating voltage for the detector and the another (50 Ω floating shield SMA-SMA) for the output signal from the detector.

Potassium-rubidium-cesium ion source
The surface ion source was attached to the entrance side of the MR-TOF chamber *i.e.* to the opposite end flange from the detector. The ion source is shown in figure 11 and it is manufactured by Heatwave Labs Inc under model number 101139. In the experimental setup here, the ion source is enclosed inside its own chamber, which also contains necessary optical elements for producing continuous ion beam: a skimmer plate and an einzel lens. The ion source and the optical elements were electrically isolated from the rest of the setup with a 5-cm long plastic insulator so that it can be floated on a high voltage potential, which will define the beam energy.

Ion source emitter material is fused into a porous indirectly heated tungsten disk welded

to the heater body. The emitter material is placed in a controlled manner to the emitter matrix and then melted into the tungsten disk surface under hydrogen atmosphere. A non-inductively wound molybdenum coil is attached to the heater, which is attached to the source body with pure Al_2O_3. The emitter matrix and the heating cavity are insulated from each other inside the molybdenum body. The source is attached to the base plate by means of a tripod that is made by soldering three rhenium supports to the body with 120 degrees spacing between each other[23].

Thermal emission, the physical phenomenon upon which the ion source is based, has been known for a relatively long time. In this case the phenomenon is realized by the emission of positive ions from a solid material. Off-line ions sources of this kind are easy to use: the ion source is heated by electric current and the material simply emits ions. For the ion source in use at IGISOL produces $^{39}K^{1+}$, $^{85,87}Rb^{1+}$ and $^{133}Cs^{1+}$ ions were chosen. In addition to ease of use the unreactivity of the ion source in the atmosphere is advantageous. These ion sources are primarily intended for low energy experiments with less than 100 eV energies where low energy dispersion is essential. At the very beginning of the heating, small quantities of impurities are present but their proportion decreases rapidly with rising emitter temperature. Precise relationship between positive ions and neutral particles emitted from the ion source is unknown, but it is apparent from the experiments that ions have a significantly greater share of the total number of particles. The absolute maximum heating current of the ion source given by the manufacturer is 1.8 amps which corresponds to operating temperature of 1100 °C and produces ion current up to 1 mA/cm^2 at best. [23]. In this thesis study the actual need for ion current was much less than the above-mentioned maximum value.

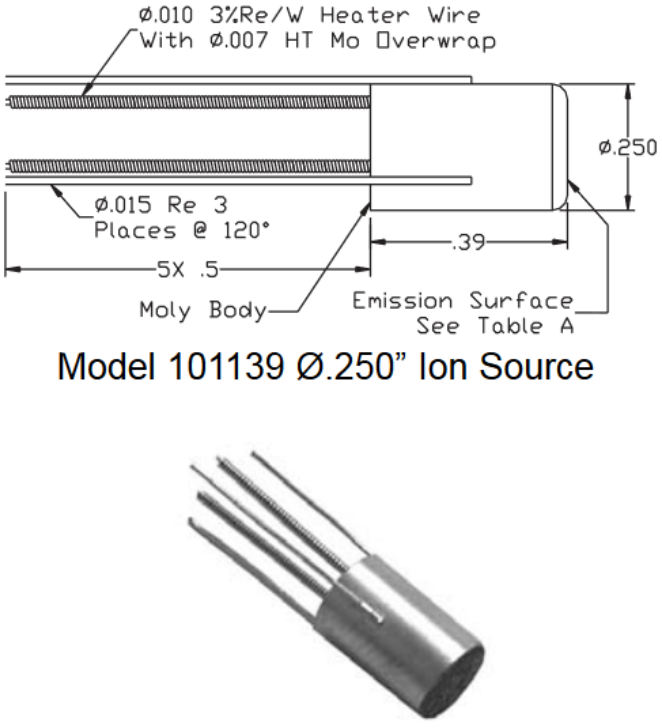

Figure 11: Surface ion source produced continuous ion beam consisting of positive singly charged potassium $^{39}K^{1+}$, rubidium $^{85,87}Rb^{1+}$ and caesium $^{133}Cs^{1+}$ ions. Figure is from [23]. The dimensions are given in inches.

Power supplies
In this work also the ISEG voltage modules assigned for MR-TOF electrostatic mirror electrodes were taken into test use. There were two standard modules and one customized version. The positive voltage supply is model EHS 8040p (8 channels, +4 kV max voltage) and the negative one is module EDS F1 30n (16 channels, max −3 kV per channel). These voltage modules were inserted into 4-module ISEG crate of type ECH 224. The voltages are controlled through a computer interface. In the test assembly built here, ISEG voltage supplies were used for applying negative operating voltage for the MagneTOF detector as well both positive and negative voltages for the Bradbury-Nielsen gate. Other power supplies used in the experimental setup were standard manually controlled laboratory instruments. A total of four supplies were needed for the off-line ion source. One was used to generate the ion acceleration voltage, another for the heating current, third for the skimmer plate voltage and the last one to focus the ion beam by using the einzel lens.

Bradbury-Nielsen gate voltage switch
Essential part of an MR-TOF setup for ion beam purification purposes, is the BNG, which can be quickly switched to either transmit or to not transmit ions. The time scale in which this voltage switching should be completed is as low as couple of tens of nanoseconds. This is the time scale ions need to pass the gate. Voltage switch model NIM-AMX-250 by CGC instruments was used to pulse the voltage on the BNG wires. It has three independent channels controlled by TTL (+5 V) logic. When the TTL signal is high (+5 V), the high voltage input is fed to the outputs of the switches and when the logic is low (0 V), ground potential is outputted. The BNG voltage switch output was tested to have a full rise time of $\sim$ 50 ns for a voltage set of $\pm$150 V at gate wires. Switching to 90 % of the set value is reached in $\sim$30 ns. Figure 12 shows BNG voltage switch output pulses measured with an oscilloscope.

Trigger pulse
A 5 V TTL trigger pulse was required for both the measurement data acquisition system and the BNG voltage switch. In this work a square pulse generated with 'Agilent 80 MHz Function / Arbitrary Waveform Generator' was chosen. The rising edge of the TTL pulse was set to start the data acquisition and the width of this pulse defined the time that the BNG was kept in open mode. The measurement cycles were repeated in accordance with the pulse rate set by the pulse generator.

Data acquisition time-to-digital converter (TDC)
In the this test setup, the MagneTOF detector output signal was passed through a 50 Ω shielded coaxial cable directly to the Time-To-Digital Converter (TDC). Since the detection threshold for the TDC is small enough to registed few mV signals, there was no need to use a fast preamplifier. The used TDC (model MCS6A) is manufactured by FAST ComTec and is known under model number MCS6A. This model has one START input for trigger pulse and one STOP input for detector output signal. The inputs are SMA type with 50 Ω impedance and their sensitivity is better than 10 mV according to detector manual. The threshold voltage of the input channels is tunable in the range of $\pm$1.5 V and the edge sensitivity may be chosen as rising, falling or both edges. The time resolution of the TDC is 256 ps at its best. The data is read out to a Windows 10 PC through a USB connector. Inputs and other characteristics of the TDC were controlled via MPANT software by FAST ComTec. Since the TDC inputs can handle maximum voltage of only 1.5 V, the 5 V trigger signal from the function generator is reduced to 1.5 V using a simple voltage divider circuit.

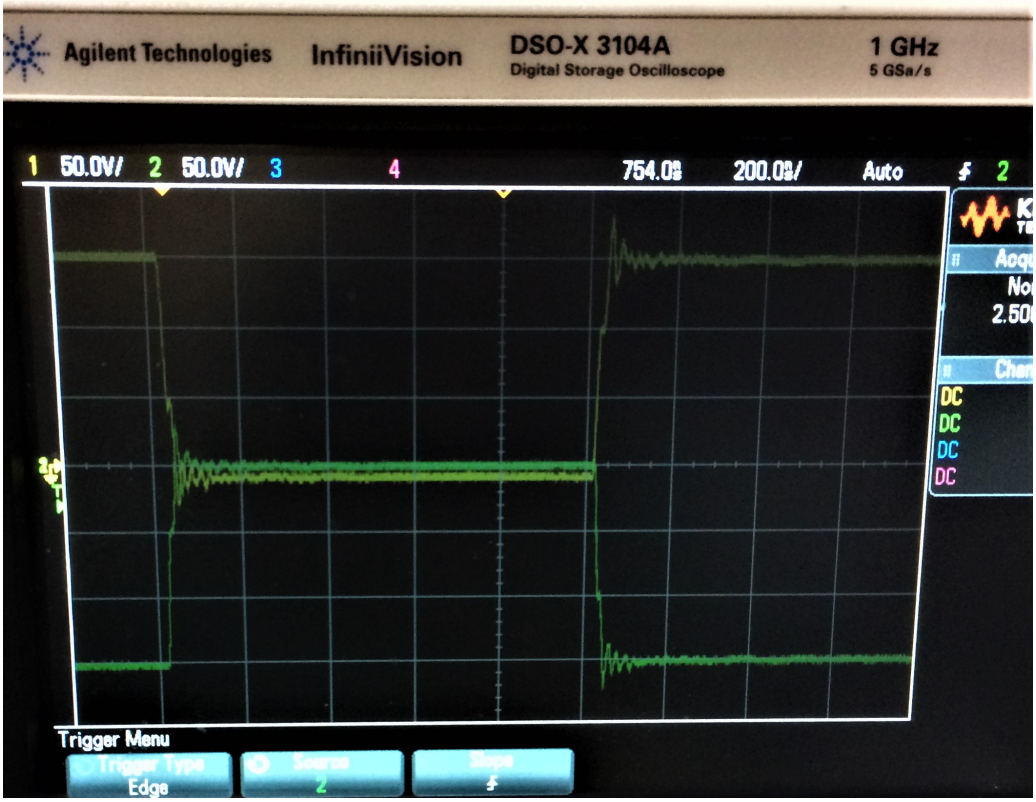

Figure 12: Voltage switch output voltage pulses visualized by oscilloscope. Voltage set ±150V was used and 90 % of the voltage set value is reached in about 30 ns.

Data acquisition procedure
The data acquisition can be summarized as follows: the rising edge of the trigger pulse starts a new cycle for the TDC ($t = 0$) and each of the ions detected with the MagneTOF detector generates a signal, whose time was recorded by the TDC. That is, in other words, the trigger pulse acted as a START signal for the measurement cycle and the ions arriving at the detector generated STOP signals that were recorded in the time-of-flight spectrum by TDC. These cycles are also called 'sweeps'.

Since the BNG voltage switch box has a fixed 380 ns delay after the start signal before the voltages are actually pulsed the trigger pulse started first the data acquisition that has no start delay and hence, after 380 ns, the BNG was switched from ±250 V to ground potential. When there is no voltage on the gate, the gate is open and ions can pass through the gate to the detector. The falling edge of the trigger pulse in turn caused BNG voltages to be switched on again, meaning that gate was turned into closed mode again and ions were not able to pass through the gate. The identical measurement cycle begins after trigger pulse period time when the new rising edge hits with the TDC for a new data acquisition and re-engages the BNG voltages as described above. Thus, depending on the ion beam intensity, certain amount of ions were able to pass through the ion gate during this well defined opening time ΔT referring to the trigger pulse width. As lighter nuclides gain higher velocity they would enter the detector first and heavier ions later in order by their mass. Figure 13 presents an example for the data acquisition routine with BNG opening time of 650 ns.

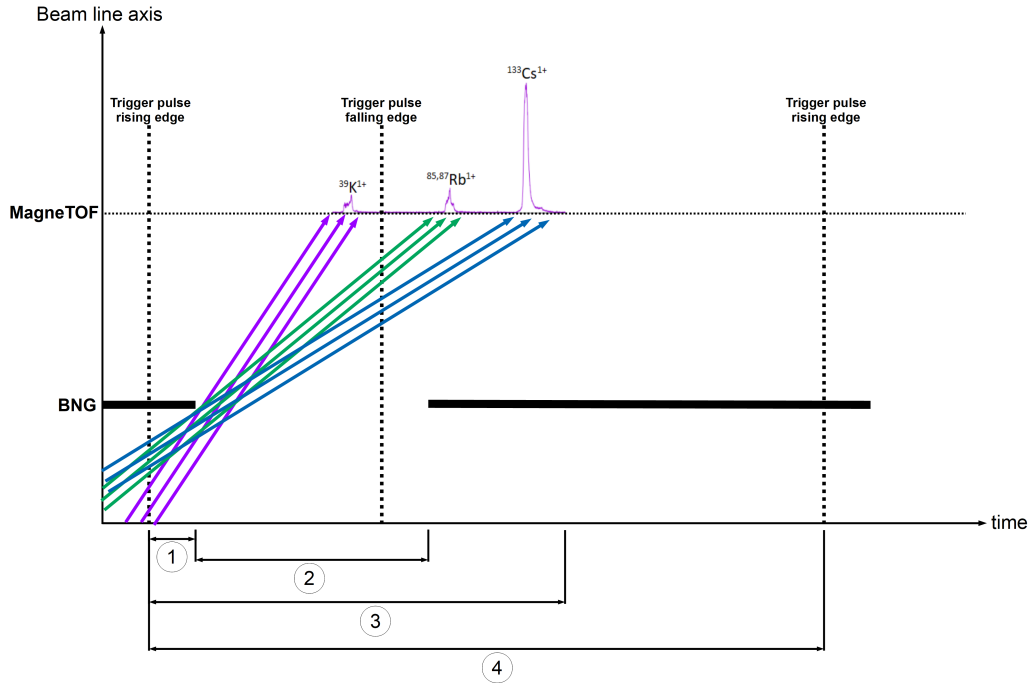

Figure 13: Schematic timing diagram presenting the data acquisition procedure. Vertical axis corresponds to beam line axis position within the MR-TOF vacuum chamber and timeline on the horizontal axis respectively. Labels are listed as follows: 1) voltage switch delay of 380 ns 2) gate open time $\Delta T = 650$ ns 3) sweep duration 64 µs 4) measurement cycle duration 10 ms. Thick black line shows the BNG closed mode and the arrows with different slopes corresponds to K, Rb and Cs ions passing through the gate with different velocities. Vertical dashed lines point out the rising and falling edges of the user-generated trigger signal.

3.2 OFF-LINE MEASUREMENTS

After setting up the experimental test station it was time to do the off-line measurements for MagneTOF commissioning and BNG characterization. Here, measurements are categorized into five groups depending on the parameters being studied. First two measurements were dedicated to the commissioning of the MagneTOF detector and the latter three focused on charaterizing the BNG by recording the ion's time of flight distribution while varying either the applied wire voltages or the gate opening time.

Measurement 1: Plateau curves
MagneTOF Application Notes written by the manufacturer ETP Ion Detect include instructions how to find the suitable detector operating voltage. The idea is to record the number of detected ions per cycle while keeping the ion source settings constant *i.e.* to have same number of ions/s emitted from the source, and then to vary the detector voltage. Plotting the ion countrate as a function of detector operating voltage produces a so called plateau curve presented in figure 14. This procedure is used not only to find out proper operating voltage at the first use of the device but also to monitor aging of the detector. Smaller voltage steps result in smoother plateau curves and operating voltages can be read with better accuracy. Applying suitable operating voltage for MagneTOF ensures sufficient output signal gain and long service life at the same time.

Measurement 2: TDC threshold voltage
The two plauteau curves published by the manufacturer are obtained with two different signal threshold voltages. Any signal higher than the TDC threshold is counted. Measuring countrates as a function of the TDC threshold will reveal the proper setting: not too low to count noise and not too high to miss some real signals. During this experiment all the off-line ion source settings, detector voltage and the number of measurement cycles are kept constant. Only the TDC threshold setting was varied. Suitable detector operating voltage was found in the middle of the plateau curve determined in the first measurement.

Measurement 3: Minimum time BNG can be open
This measurement category aims at answering what is the minimum time the gate needs to be open so that ions with a certain temporal width are able to pass through the BNG. Additionally, the rising and falling edges of the ion pulses in the spectrum reveal how fast the gate really is *i.e.* how long does it take to switch from open mode to closed and vice versa. Here the number of detected ions as a function of time is recorded while varying the trigger pulse width, which changes the opening time of the BNG. Voltages for both wire sets are the same in amplitude but opposite in polarity when the gate is "closed". This is denoted as symmetric BNG voltages.

Measurement 4: Voltage required to sufficiently deflect ions
Work with symmetric BNG voltages continues by studuying in practice the relation between deflection angle of incoming ions and gate voltages presented in equation 8. As voltages are changed step by step the number of ions entering the detector are observed. By comparing ion countrates during gate open and closed states one can determine what is the deflection angle that manages to block the ions so that they don't reach the detector.

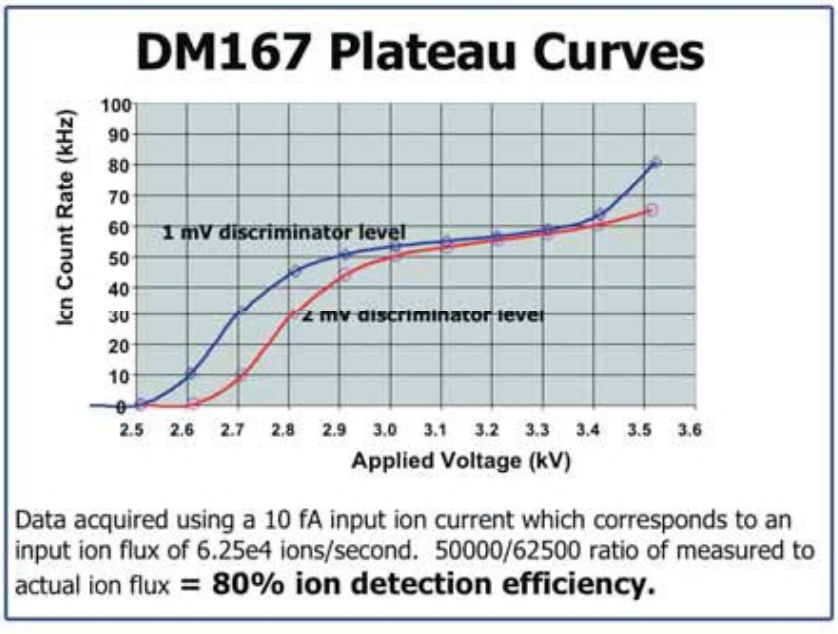

Figure 14: Manufacturer's example of how to determine the operating voltage of the MagneTOF detector. Note that the detector characterized in this graph is under model number DM167 and the device commissioned at IGISOL is DM291, respectively, though the principle for determining the operating vooltage is the same. Further information on different MagneTOF features and this figure can be found in Ref. [7]

Measurement 5: Asymmetric voltages
In addition to symmetric gate voltages the BNG can also be studied with asymmetric voltages on the wires. Motivation for this measurement category was learned from the BNG characterization study at TRIUMF [22]. This measurement aims at learning more about gate's time focussing and de-focussing effects presented in figure 15. Time focusing produces two high-intensity peaks on both edges of the ion pulse and in turn the de-focusing causes pulses with more rounded shape. In practice this experiment is carried out by keeping the voltage difference between the two wire sets constant $\Delta \mathrm{V} > 0$. Measurement starts with one of the wire sets at zero potential, which now may be chosen as $V_{pos} = 0$ V. The other wire set has potential corresponding to the voltage difference chosen, thus now we have $V_{neg} = -\Delta \mathrm{V}$. Both of the wire voltages are changed with equal steps so that always ΔV remains betwen the wires from measurement run to another. Half way through the voltages meet each other in amplitude but are opposite in polarity *i.e.* the midmost of the measurement runs is done again with symmetric voltages $V_{neg} = -\Delta|V|/2$ and $V_{pos} = +\Delta|V|/2$. Finally, in the last measurement cycle the gate ends up to a state in which it has voltages $V_{pos} = +\Delta \mathrm{V}$ and $V_{neg} = 0$ V.

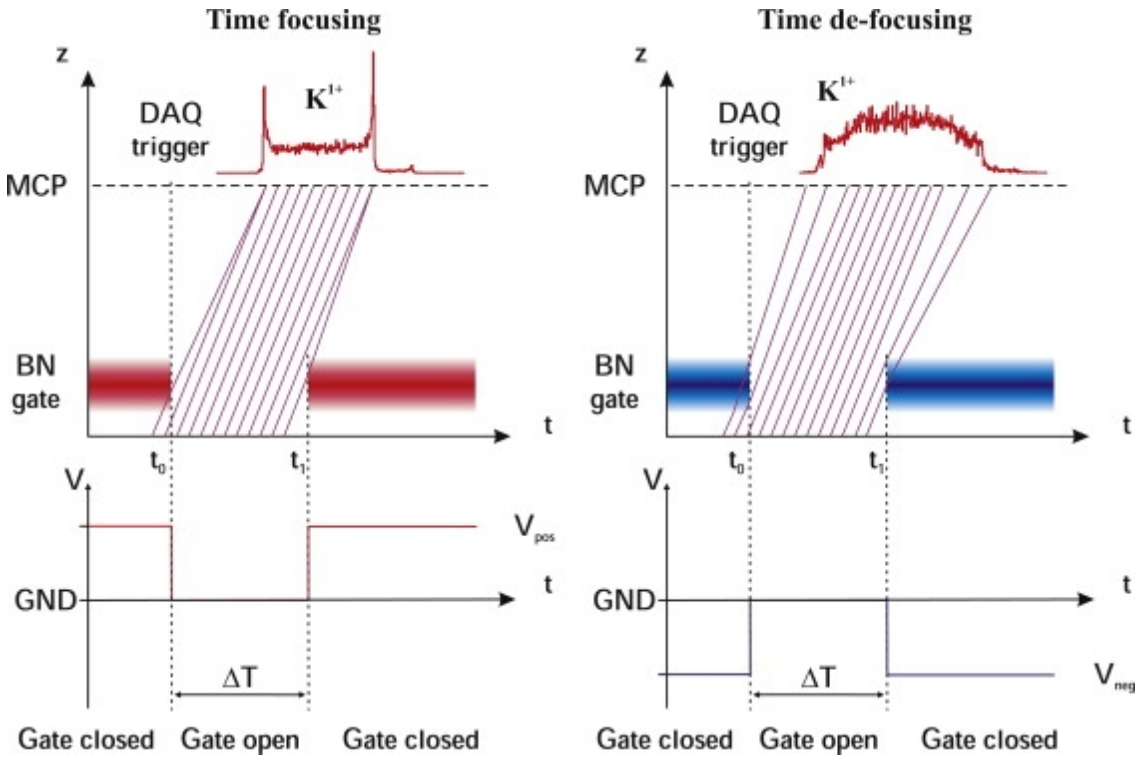

Figure 15: Illustration of the time focus phenomenon. Gate voltages are shown at the bottom. The slope of the lines inserted visualises the velocity of ions. Time focusing results in two intense peaks at both sides of the ion pulse and in de-focusing mode the opposite effect is observed. Figure is taken from Ref. [22].

4 RESULTS

4.1 COMMISSIONING OF THE NEW MAGNETOF DETECTOR

The new MagneTOF detector mounted inside the exprimental setup was first tested and characterized by measuring countinuous beam of singly charged ^{39}K, ^{85,87}Rb and ^{133}Cs ions extracted from the surface ion source. Since the detector was never used before, its operating voltage was gradually increased starting from lower values while letting the detector to settle between voltage increments. Beam intensity was also gradually increased to test detector's response to increased number of ions.

First way making sure that the detector is working as expected was to check the detector output signal form by using an Agilent Technologies oscilloscope, model DSO-X 3104A, 1 GHz. With 1.0 A heating current and 400 V accelerating voltage the ion source produced moderate intensity beam and about 110 ions/s were detected with the MagneTOF detector. At this point detector's operating voltage was brought only up to -1700 V. According to detector manual, this would lead to output signal with height of 30 mV into 50 Ω and ∼ 1 ns width. An example of a signal with these settings is shown in figure 16.

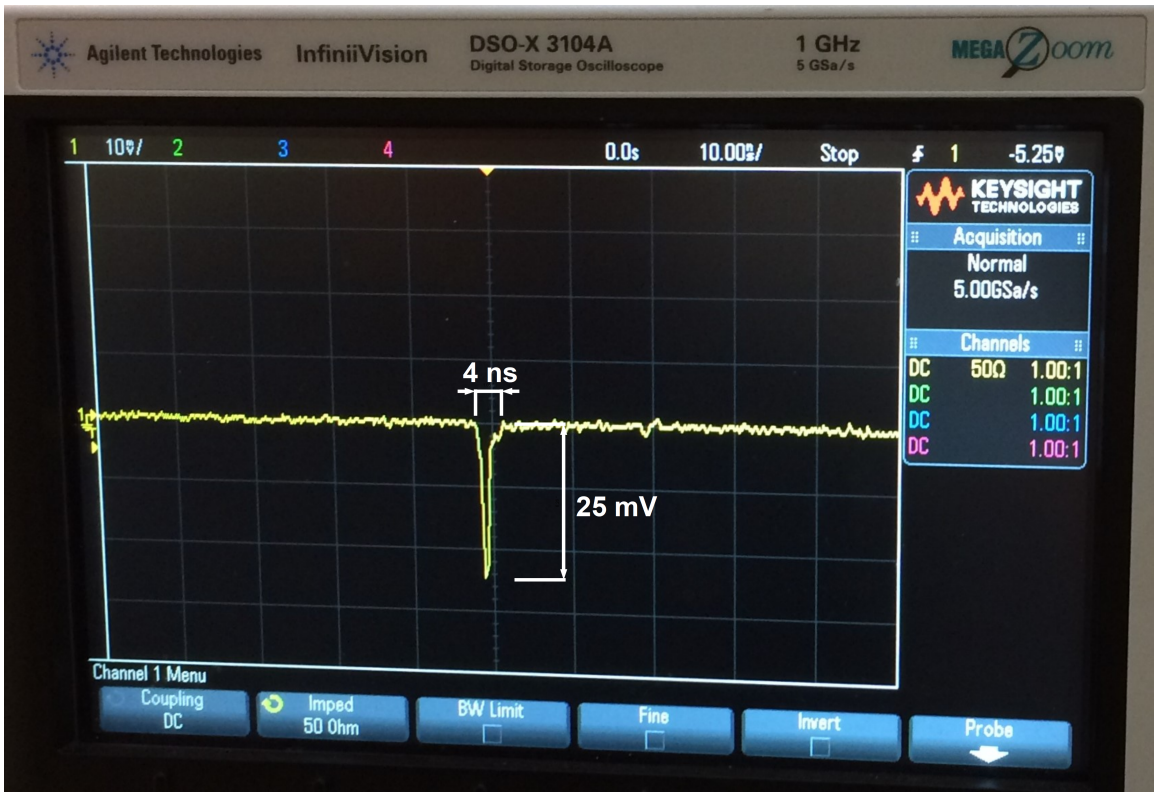

Figure 16: Ion signal from MagneTOF detector measured with Agilent DSO-X 3104A oscilloscope.

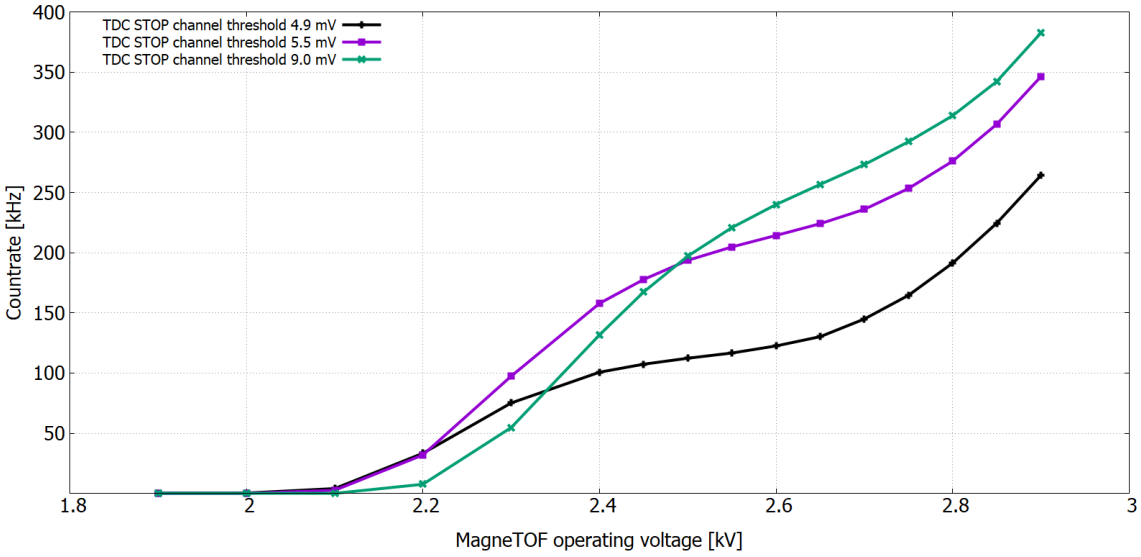

Figure 17: IGISOL MagneTOF DM291 Plateau curves with three different TDC STOP channel threshold settings.

Next, the suitable operating voltage range for the detector was measured. This test was denoted as 'measurement 1' earlier in section 3.2. Pressure in the vacuum chamber was 2.92×10^{-8} mbar, orders of magnitude better than required to safely work with the detector. Ion source settings were adjusted by increasing the heating current up to 1.1 A. Beam energy was kept about the same as above, 410 eV. Data acquisition system consisting of the TDC device and the MPANT software was used and number of switching cycles was set to 1000 repetitions with frequency of 100 Hz. The operating voltage of the detector was increased from 1.9 kV up to 2.4 kV with step size of 100 V and from 2.4 kV up to 2.9 kV with step size of 50 V. The total number of ions detected by MagneTOF was recorded for each operating voltage set value. The time for one sweep *i.e.* measurement cycle was $\sim$ 9.86 ms hence the countrate was calculated by dividing that total number of detected ions with the total duration of 1000 sweeps (9.86 s). Countrates as a function of operating voltages are show in figure 17. The measurement was repeated with several different TDC STOP channel threshold settings. The three curves presented are the so called plateau curves with TDC STOP channel threshold voltages of 4.9 mV, 5.5 mV and 9.0 mV. Suitable operating high voltage can now be determined by moving up along the curve above the "knee" which refers to the voltage range where small voltage deviations do not cause significant changes at the countrate levels. For the new detector commissioned here, the suitable operating voltage settled into a range between 2600 V and 2700 V.

As the commisioning of the detector continued, higher ion currents were used. The second measurement set for this purpose consisted of countrates recorded as a function of TDC device STOP channel threshold voltage setting. Ion source heating current was set to 1.319 A with accelerating voltage of 410 V. Data acquisition system settings were kept the same as in measurement 1 described above. The MagneTOF detector operating voltage was chosen to have 2650 V set value. The TDC STOP channel that was used for measuring time-of-flight for ions was controlled via MPANT software. By changing the threshold voltage and recording corresponding countrate levels the curve in figure 18 was obtained. The steep, rising edge at 5-8 mV is explained by the fact that, with less than 5 mV threshold voltages, the TDC device can not distinguish the signal to be measured

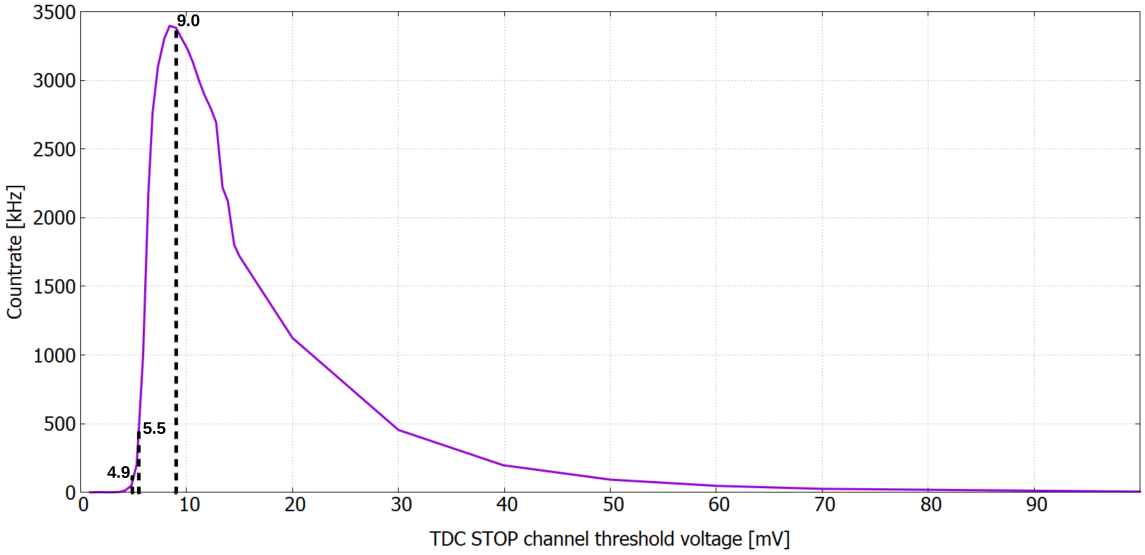

Figure 18: Detected ion countrate as a function of TDC STOP channel threshold voltage. The three threshold voltage settings used to measure data in Fig. 17 are indicated.

from the background noise. By choosing the threshold voltage setting that produces the highest ion countrate level, the detection efficiency is maximized. Also this measurement was repeated multiple times and from the resulting curves it shows that for this system the STOP channel threshold should be set close to -8.4 mV.

4.2 JYFLTRAP BNG PROPERTIES

With suitable MagneTOF and TDC settings determined above it was time to characterize the BN gate, see chapter 3.2 measurements 3,4 and 5.

Firstly, the surface ions source settings were modified in order to increase the ion beam intensity. Heating current was set to 1.3 A and at the same time the einzel lens voltage was optimised in order to focus the beam to the BNG. With these settings the ion source produced a beam that resulted in 2.8 million ions/s detected by the MagneTOF. Also the accelerating voltage of ions was brought up to 1500 V as it will be close to the energy to be finally used with the MR-TOF.

MagneTOF detector was set to operating voltage of -2650 V and the TDC STOP channel threshold voltage was set to -8.4 mV. Measurement cycles were repeated with frequency of 100 Hz for total number of 25000. A time-of-flight spectrum of ions was recorded using 3.2 ns as the binwidth in the MPANT software. The BNG had symmetric voltages of $\pm$ 250 V supplied from the ISEG power supply through the voltage switch as described earlier in section 3.1.

In measurement 3, the minimum time the gate can be opened so that incoming ions are able to pass through it and reach the detector was studied. It was realised by recording time-of-flight distribution of ions with different trigger pulse width settings. Measurement series was started with 30 ns gate opening time followed by 10 ns increment in trigger pulse width up to 300 ns set value. From there, 50 ns step size was used up to 1 µs pulse width. Results are summarized in figure 19. With gate opening times $\Delta T \leq 120$ ns ions did not reach the detector. Trigger pulse widths longer than 120 ns resulted in three bunches of ions separated in time based on their differences in mass. The first ions to

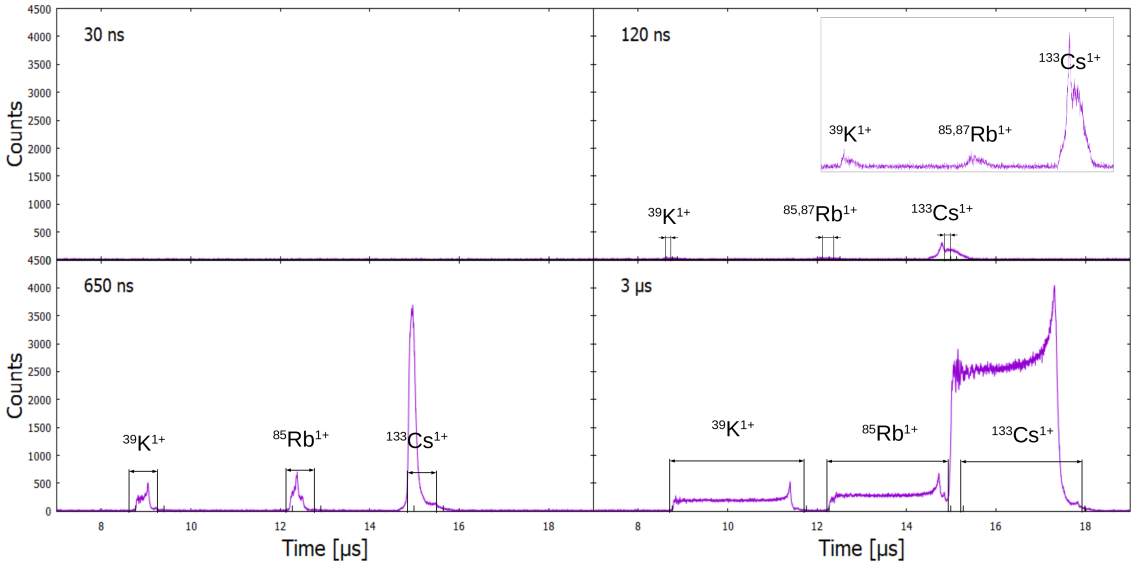

Figure 19: Time of flight spectrums with different gate-open pulse widths. See text for further explanation.

reach the detector were potassium nuclides, second bunch consisted of rubidium and the final caesium. As seen from in the figure, also the isotope intensities differed. The ion beam was dominantly composed of $^{133}Cs^{1+}$, the second largest fraction being $^{85,87}Rb^{1+}$ ions and the smallest fraction $^{39}K^{1+}$ ions. As an additional test the trigger pulse width was increased until peaks were seen to overlap at gate opening time of 3 µs.

Investigations on symmetric BNG voltages continued in measurement 4. This time it was about the voltages required to block the incoming ion beam sufficiently. At this point vacuum conditions had further improved to 1.56×10^{-8} mbar level. The surface ion source and the TDC settings were kept the same as in measurement 3 described earlier. One cycle was set to be 10 ms long, and the BNG was set to be open for 1 µs during the cycle. Starting from ±50 V in steps of 10 V the voltage at the wires was increased up to ±250 V setting. It turned out that with voltages more than ±140 V the gate does not transmit any ions, *i.e.* it is fully closed. Figure 20 shows four of the resulting spectrums in this measurement category. The first two spectrums from the left had BNG voltage sets of ±50 V and ±100 V. The background levels of ions detected are relatively high indicating that ions are able to enter the detector at all times including the gate closed mode with wire voltages switched on. The third time-of-flight spectrum in figure 20 had voltage set of ±150 V and it shows that the gate can already be interpreted as fully closed with negligible background. The last measurement run was done with the highest voltage set of ±250 V. Although in this measurement category symmetric BNG voltages were used, there are some time focusing effect visible in the time-of-flight spectrums. With voltages under ±100 V there is higher intensity on the rising edge of the ion pulses whereas with voltages over ±150 V there is a peak at the falling edge of the pulses.

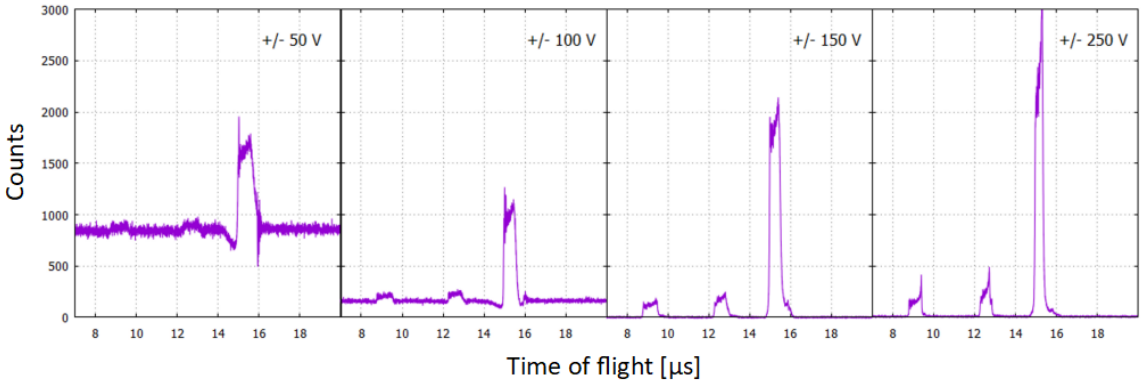

Figure 20: Symmetric voltages required for sufficient deflection angle of ion trajectories.

In practice it is best to use as high voltages as possible to maximally deflect the ions. Symmetric voltages are obvious choice for this, voltage switch switching range can then be maximally utilized. It is also useful to investigate how asymmetric voltages affects the time focus of the edges, listed as 'measurement 5' earlier in this thesis report. Ion source settings and TDC data acquisition system settings were not changed from previous two measurements. The voltage difference between the positive and negative set of wires was kept as constant $\Delta V = 250$ V. Initial settings were given as: $V_{POS} = 250$ V and $V_{NEG} = 0$ V. The positive voltage was reduced and the negative one was increased in steps of 25 V meaning that the BNG reached symmetric voltages again at $\pm$ 125 V. This procedure was continued until the voltage settings of the system were opposite to the initial *i.e.* $V_{POS} = 0$ V and $V_{NEG} = -250$ V. Figure 21 illustrates the time focus phenomenon observed in this measuremet category. The three columns of the figure each represent one nuclide pulse so that the leftmost of columns is composed of potassium ions, rubidium is in the middle and cesium on the right side. Each row presents a different asymmetric voltage setting. In the two top rows, the net voltage $V_{NET} = V_{POS} + V_{NEG}$ of the gate wires was negative, in the middle row the gate had symmetrical voltages ($V_{NET} = 0$) and respectively in the two lower rows the net voltage was positive. As it is seen from the previous 'measurement 4', the symmetric voltage set of $\pm$ 125 V is just under the voltages required to deflect ions sufficiently.

Symmetric BNG wire voltages produce small deflection region as it was presented earlier in section 2.2.4. Now, with wire spacing of $d = 500$ µm the deflection region for symmetric voltage configuration becomes $2d = 1$ mm. Asymmetric voltages create a potential field that extends further out. Depending on the applied net potential V_{NET} the potential field has an accelerating or retarding effect on the incoming ions when the ions fly near the gate when the voltage is switched. With the gate used, it appears that with $V_{NET} < 0$ ion pulses have more rounded shape which points out the time de-focusing effect. Settings $V_{NET} > 0$ produce ion pulses with more angular shape which refers to time focusing phenomenon.

Dimension lines in the middle row spectrums show the calculated time-of-flight for each isotope. Equation 3 presents the phenomenom of charged particles moving within an electric field. The time-of-flight for ions can be solved as the distance between the BNG and the detector is known $s = 0.635$ m and this abovementioned equation can be applied in these tests as the ions are always at ground potential while flying between the BNG and the detector. According to equation 11 the residence time, meaning the time needed

for an ion to pass through the BNG deflection region, results as follows: (^{39}K) 11.6 ns, (^{85}Rb) 17.1 ns, (^{87}Rb) 17.3 ns and (^{133}Cs) 21.4 ns.

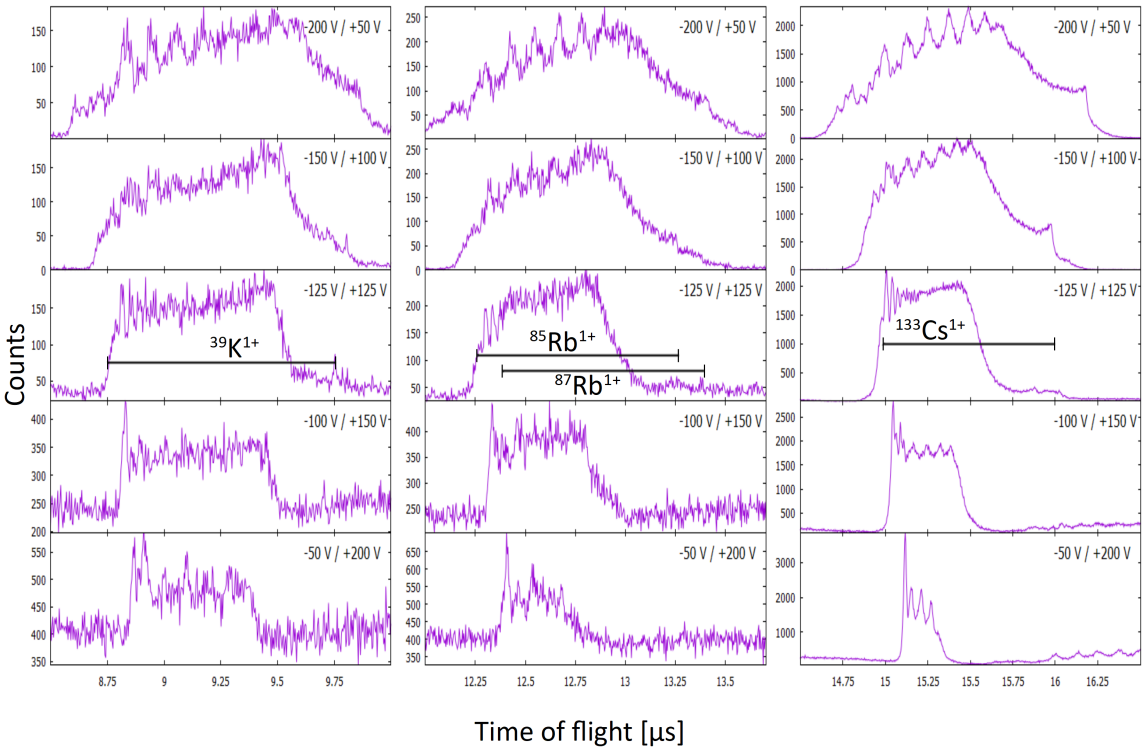

Figure 21: Ion pulses detected by applying asymmetric voltages on the gate wires. The time de-focusing effect (less sharp edges) can be seen at the two top rows while the net potential on gate wires is negative. Time focusing changes when the net potential turns into positive at the bottom.

5 DISCUSSION

The aim of the study was to successfully commission the new MagneTOF ion detector and the Bardbury-Nielsen ion gate. More specifically, the goal was to characterize how well the in-house produced BNG performs, especially how fast the gate goes from fully-transmitting mode to fully-closed mode. In addition to this, the construction phase of the MR-TOF project started as well. Both the MagneTOF detector and the BNG will finally be installed in the extraction chamber of the MR-TOF device and therefore this work will provide essential information on properties of these devices.

Setting up the off-line test station was a rather straightforward process. Most of the components like vacuum pump, chamber, flanges etc. reserved for the MR-TOF assembly could be utilized. The only exception were the brackets designed for mounting the detector and the BNG inside the MR-TOF vacuum chamber. Since both the detector and the off-line ion source required high voltages, special attention was paid to electrical insulation and that each component of the setup is in some defined potential and not left floating. All the parts installed inside the vacuum chamber were made out of ultra high vacuum compatible and bakeable materials, cleaned and polished enough to produce a suitable level of vacuum in the 10^{-8} mbar range and below. The off-line test station was built at a temporary location in the IGISOL hall. For the actual MR-TOF, the aim is to have vacuum on the order of 10^{-10} mbar to optimize the conditions for mass separations and measurements. With careful preparation and baking all the parts and the vacuum chamber, this goal is achievable.

The MagneTOF detector was conditioned by moderately increasing the operating voltage step by step. Continuous beam of potassium, rubidium and caesium ions was extracted from the surface ion source. Detector output signals matched excellently the expectations given by the manufacturer. As a result, clean negative 1-ns pulses with an amplitude of about 25 mV into 50 Ω were obtained. Setting the operating voltage of the detector to the correct value ensures that each signal is counted only once with maximal detection effiency and long service life at the same time. The data acquisition system included the MagneTOF detector and the TDC, which was controlled via MPANT software.

Measured plateau curve shape for MagneTOF DM291 matched the shape given by the manufacturer. Based on the results obtained in this work, the appropriate operating voltage value was found in the range of 2600 V and 2700 V, which is a well expected initial state for a new unused MagneTOF detector. The TDC device has two inputs channels. The START channel receives the user generated trigger pulse and the STOP channel is used for recording ion's time of flight. Threshold and polarity for both channels can be set through MPANT software. Ion countrates were investigated as a function of the STOP channel threshold voltage. In principle, the case would be that the ion countrate grows as the TDC STOP channel threshold voltage approaches zero. This is because all MagneTOF output signals with amplitudes under the threshold set value are not counted by the TDC. However, with threshold setting under 5 mV the TDC device apparently has difficulties to separate the real pulses from the background noise since the rate of STOP

signals starts to decrease. It must be for that reason that the countrate goes to zero when the TDC STOP channel threshold value is set below 5 mV as it was presented earlier in section 4. This behaviour explains why the measured plateau curve with 9.0 mV TDC threshold setting is higher in ion countrates compared to the second curve with 5.5 mV and the third curve with 4.9 mV threshold voltage and not the other way around as it perhaps intuitively could thought to be.

The stability of the ion source was evaluated by repeated measurements with identical TDC settings. The number of ions detected within a time interval *i.e.* the intensity of the beam was recorded. Variations were always found to be less than 3 % of the observed mean intensity. Thus, the continuous ion beam produced by the source is considered to be sufficiently stable for BNG characterization. The ease-of-use and reliable operation of the ion source enabled the construction of a compact off-line test station. The ion beam focus was modified by varying the voltages controlling the ion-optical devices. Optimizing these settings was not a critical or limiting factor in this work since the ion beam intensity was big enough to obtain the required statistical sample size. On the other hand, it must be noted that the ion beam was not very coherent which can be seen especially in the experiment investigating asymmetric gate voltages.

Continuous ion beam was pulsed with IGISOL-manufactured BNG by varying both the voltage applied to gate wires and the gate opening times. Since the MR-TOF device is to be used for ion beam purification *i.e.* separating ions of interest from contaminant particles, the most important thing was to find out how fast the BNG is. This was studied by modifying the width of the user generated trigger pulse, which directly defined the gate opening time. As a result, the gate was able to separate the potassium, rubidium and cesium isotopes with gate opening times of 120 ns. Initially the aim was to have successful BNG operations with gate opening times under 50 ns. So, the result gained here is a promising one but also leaves room for further development.

Bradbury-Nielsen ion gate properties are most affected by the material of its electrodes, the diameter of the wires and the wire spacing. In this thesis report variables affecting the gate properties are presented. Equation 10 presented earlier in section 2.2.4 results in 7.1 pF as the theoretical capacitance of the gate. This goes well in line with the reference values found in the literature for BNGs with similar purpose of use. If ions fly within the deflection region while gate voltages are being switched only partial deflection is achieved. Thus, the residence times mentioned earlier in section 4.2 determine the theoretical maximum time resolution of the gate presented in this work. The maximum error on wire spacing was measured to be under 10 µm.

Another experiment with symmetric gate voltage configuration was done in order to systematically study the deflection angles of incoming ions. With lower voltages starting from set values of ± 50 V the ions were able to pass through the gate at all times *i.e.* the gate was not able to block the incoming ion beam. This was seen as a high background countrates in the time-of-flight spectrums. Even with this low voltage set the BNG deflects the incoming ion beam with some small angle. When the voltage set was brought close to ± 140 V the background of the spectrum nearly vanishes. This corresponds to deflection angle of 2.4 degrees derived from equation 8 presented earlier in section 2.2.4.

Open and closed modes of the BNG were defined by the voltage switch. Thus, the time interval in which the voltages are successfully switched on and off is particularly important. In addition to the rise time of the voltage pulses, fluctuations are also undesirable for the

ideal operation of the gate. The switch box was taken as close to the gate position as possible allowing the negative and positive voltages to be transmitted to the gate wires using short SHV cables. The measured voltage rise time at gate wires was about 25 ns with voltages set to ± 150 V needed for sufficient deflection. Trigger pulses and MagneTOF output signals should be transferred only by appropriate coaxial cables in order to signal attenuation and reflections. Care was taken to have the whole signal line from MagneTOF detector to the TDC 50 Ω. The voltage switch caused unavoidable noise during the swithching and these interferences were visible in the time-of-flight spectrums measured.

The standard operation principle of the BNG is based on symmetrical wire voltages in order to minimize edge time focusing and defocusing effects. However, in this work, asymmetric BNG voltages were investigated to gain more information about the time focus phenomenon observed in the time-of-flight spectrums. The time de-focusing effect on ion pulses were observed when the net wire voltage was negative. This phenomenon was revealed by the shape of measured ion pulses in the time-of-flight spectrum. The pulses were wider and rounded in shape on the edges. Ion countrate fluctuations visible in the spectrums are due to the fast voltage switch. In turn, the time focusing mode was investigated by applying positive net voltages. Although, the phenomenon could not be detected as clearly as the abovementioned de-focusing effect. With positive net voltages the ion pulses had steeper rising and falling edges. However, the expected two high intensity peaks at both edges of the pulse were not observed in this set of measurements. Instead, only one peak at the rising edge of the pulse was observed.

Time-of-flight spectrums resulting from asymmetric gate voltages demonstrate the angular dispersion effect in BNG operations. Ions that pass the BNG set to non-transmitting mode in a non-perpendicular angle may experience focusing effect that guides them towards the detector or, on the contrary, ions might be de-focused away from the detector input aperture. With negative net wire voltage there is a residual peak in the falling edge of the pulse whereas with positive net wire voltage there is a low-intensity tail instead. It could be deduced that the angular deviation of the ions is such that the negative net voltage on wires focuses ions towards the detector and positive net voltages deflect ions away from it. During the measurement series investigating asymmetric gate voltages the midmost of the repetitions was carried out again with symmetric configuration at voltages of ± 125 V which, unfortunately, was not quite enough to completely block the incoming ion beam when the gate is closed but this way the switching effects are more pronounced.

In addition, the measured time-of-flight for ions was compared to theoretical expectations. It turned out that the first ions to arrive to the detector after the gate is opened have almost exactly the calculated time-of-flight. However, the measured pulse width did not match the user defined trigger pulse width. Some of the pulses were too narrow in width as the shape of the falling edge was not ideal *i.e.* when the gate was closed, ions were observed much later than their expected time-of-flight. The possible benefit of BNG operations at asymmetric voltage configuration could be achieved in cases where the time focusing phenomenon is used for enhancing the time resolution of different ion isotopes. As mentioned, this would of course cause an increase in energy dispersion which is an unwanted feature in high precision mass measurements but probably still tolerable.

In this thesis, experimental work was considered as a part of the MR-TOF project. The purpose of this work was to start practical construction work on this project, based

on past computer simulations and design work. Overall, the results obtained in these measurements meet the aim of the study. The next steps in the construction and testing of MR-TOF assembly are already underway. The necessary modifications to the RFQ extraction side properties are examined by simulations before moving on to a set of new off-line tests. While writing this thesis report the MR-TOF electrostatic mirrors are ready for test use and the equipment is assembled in such a way that it can be moved from one measurement location to another. It would be highly benefitial to perform off-line measurements by studying ion beam in a pulsed form instead of a chopped continuous beam. For this purpose the MR-TOF setup will be installed into IGISOL beam line after the RFQ which produces ion pulses as it does in all JYFLTRAP operations. The off-line surface ion source produces positive singly charged ions the same way it did in this work and the MR-TOF device can be tested in conditions matching the final purpose of use in ion beam purification and mass spectrometry.

REFERENCES

[1] K. Blaum *High-accuracy mass spectrometry with stored ions.* Physics Reports 425 (2006) 1-78, URL https://www.sciencedirect.com/science/article/pii/S0370157305004643

[2] H. Wollnik. *History of mass measurements in time-of-flight mass analyzers.* International Journal of Mass Spectrometry 349-350 (2013) 38-46, URL http://www.sciencedirect.com/science/article/pii/S1387380613001504

[3] R.N. Wolf, D. Beck, K. Blaum, et al. *On-line separation of short-lived nuclei by a multi-reflection time-of-flight device.* Nuclear Instruments and Methods in Physics Research, Section A 686 (2012) 82, URL http://www.sciencedirect.com/science/article/pii/S016890021200575X

[4] R.N. Wolf, D. Beck, K. Blaum, et al. *ISOLTRAP's multi-reflection time-of-flight mass separator/spectrometer.* International Journal of Mass Spectrometry and Ion Processes 349-350 (2013) 123-133, URL http://www.sciencedirect.com/science/article/pii/S1387380613001115

[5] W.R. Plass, T. Dickel, C. Scheidenberger. *Multiple-reflection time-of-flight mass spectrometry.* International Journal of Mass Spectrometry and Ion Processes 349-350 (2013) 134-144, URL http://www.sciencedirect.com/science/article/pii/S138738061300239X

[6] P. Schury, M. Wada, Y. Ito, et. al. *A multi-reflection time-of-flight mass spectrograph for short-lived and super-heavy nuclei.* Nuclear Instruments and Methods in Physics Research Section B 317 (2013) 537.543, URL http://www.sciencedirect.com/science/journal/0168583X

[7] D. Stresau, K. Hunter, W. Sheils, P. Raffin, Y. Benari. Technical article: *A New Class of Robust Sub-nanosecond TOF Detectors with High Dynamic Range.* ETP, Sydney, Australia. Presented at the 54th ASMS Conference on Mass Spectroscopy, Seattle, Washington, 2006. URL https://www.etp-ms.com/file-repository/26

[8] G.W. Goodrich, W.C. Wiley. *Resistance Strip Magnetic Electron Multiplier.* Review of Scientific Instruments 32 (1961) 846-849, URL https://doi.org/10.1063/1.1717528

[9] J.L. Wiza. *Microchannel plate detectors.* Nuclear Instruments and Methods 162 (1979) 587-601, URL http://www.sciencedirect.com/science/article/pii/0029554X79907341

[10] N.E. Bradbury and R.A. Nielsen. *Absolute Values of the Electron Mobility in Hydrogen.* Physical Review 49 (1936) 388-393

[11] R. Weinkauf, K. Walter, C. Weickhardt, U. Boesl, E.W. Schlag. *Laser Tandem Mass Spectrometry in a Time of Flight Instrument.* Naturforsch Teil A 44 (1989) 1219-1225

[12] I.D. Moore, P. Dendooven, J. Ärje. *The IGISOL technique - three decades of developments.* Hyperfine Interact 223 (2014) 17-62, URL https://link.springer.com/article/10.1007/s10751-013-0871-0

[13] A. Nieminen, P. Campbell, J. Billowes, D.H. Forest, J.A.R. Griffith, J. Huikari, A. Jokinen, I.D. Moore, R. Moore, G. Tungate, J. Äystö. *On-Line Ion Cooling and Bunching for Collinear Laser Spectroscopy.* American Physical Society, Phys. Rev. Lett. 88 (2002) 094801, URL https://link.aps.org/doi/10.1103/PhysRevLett.88.094801

[14] A. Nieminen, J. Huikari, A. Jokinen, J. Äystö, P. Campbell, E.C.A. Cochrane. *Beam cooler for low-energy radioactive ions.* Nuclear Instruments and Methods in Physics Research Section A: Accelerators, Spectrometers, Detectors and Associated Equipment 469 (2001) 244-253, URL http://www.sciencedirect.com/science/article/pii/S0168900200007506

[15] V.S. Kolhinen, T. Eronen, et al. *Recommissioning of JYFLTRAP at the new IGISOL-4 facility.* Nuclear Instruments and Methods in Physics Research Section B 317 (2013) 506, URL http://www.sciencedirect.com/science/article/pii/S0168583X13008641

[16] R.N. Wolf, G. Marx, M. Rosenbusch, L. Schweikhard. *Static-mirror ion capture and time focusing for electrostatic ion-beam traps and multi-reflection time-of-flight mass analyzers by use of an in-trap potential lift.* International Journal of Mass Spectrometry 313 (2012) 8-14, URL http://www.sciencedirect.com/science/article/pii/S1387380611004775

[17] A.D. Cutter, K.L. Hunter, P.J.K. Paterson, R.W. Stresau. Technical article: *The "AGING" Mechanism in Electron Multipliers and Operating Life.* ETP Ion Detect. Presented at the 42nd ASMS Conference on Mass Spectroscopy and Allied Topics May 29-June 3, 1994, Chicago, Illinois. URL https://www.etp-ms.com/file-repository/15

[18] I.A. Zuleta, G.K. Barbula, M.D. Robbins, O.K. Yoon, R.N. Zare. *Micromachined bradbury-nielsen gates.* Analytical chemistry 79 (2007) 9160-9165, URL http://pubs.acs.org/doi/abs/10.1021/ac071581e

[19] O.K. Yoon, I.A. Zuleta, M.D. Robbins, G.K. Barbula, R.N. Zare. *Simple template-based method to produce bradbury-nielsen gates.* Journal of the American Society for Mass Spectrometry 18 (2007) 1901-1908, URL http://www.sciencedirect.com/science/article/pii/S1044030507006368

[20] O.K. Yoon, I.A. Zuleta, J.R. Kimmel, M.D. Robbins, R.N. Zare. *Duty cycle and modulation effiency of two-channel hadamard transform time-of-flight mass spectrometry.* Journal of the American Society for Mass Spectrometry 16 (2005) 1888-1901, URL http://www.sciencedirect.com/science/article/pii/S1044030507006368

[21] N.N. Rao. *Elements of Engineering Electromagnetics.* Prentice Hall: Englewood Cliffs, NJ, 1977, page 422

[22] T. Brunner, A.R. Mueller, K.O'Sullivan, M.C. Simon, M. Kossick, S. Ettenauer, A.T. Gallant, E. Mane, D. Bishop, M. Good, G. Gratta, J. Dilling. *A Large Bradbury Nielsen ion gate with flexible wire spacing based on photo-etched stainless steel grids and its characterization applying symmetric and asymmetric potentials.* International Journal of Mass Spectrometry 309 (2012) 97-103, URL `http://www.sciencedirect.com/science/article/pii/S1387380611003770`

[23] HeatWave Labs, Inc., *TB-118 Aluminosilicates Ion Sources.* Website, URL `http://www.cathode.com`, accessed 6.4.2018